



Heat flow modelling in the Transylvanian basin: Implications for the evolution of the intra-Carpathians area



Marius Tiliță^{a,b,*}, László Lenkey^c, Liviu Mațenco^a, Ferenc Horváth^c, Gergely Surányi^d, Sierd Cloetingh^a

^a Utrecht University, Faculty of Earth Sciences, Budapestlaan 4, 3584CD Utrecht, The Netherlands

^b Repsol Exploración S.A., Mendez Álvaro 44, 28045 Madrid, Spain

^c Eötvös Loránd University, Department of Geophysics and Space Science, Pazmany Peter setany 1/c, 1117 Budapest, Hungary

^d MTA-ELTE Geological, Geophysical and Space Sciences Research Group, Hungarian Academy of Sciences at Eötvös Loránd University, Pazmany Peter setany 1/c, 1117 Budapest, Hungary

ARTICLE INFO

Keywords:

Thermal structure
2D finite element thermal modelling
Dynamic topography
Transylvanian Basin
Cold back-arc basins

ABSTRACT

The evolution of sedimentary basins and their thermal structure are the result of the coupling between shallow crustal and deep lithospheric - mantle processes. When sources of shallow crustal deformation are not detectable, then deep lithospheric processes have the role to reveal the origin of these events. A particular method of investigating these deep processes is to evaluate their lithospheric thermal imprint, in particular when anomalous thermal values are exhibited. One such example is the Transylvanian Basin situated at the interior of the highly bended Carpathians chain, which shows lower heat flow values when compared with average cratonic values and even lower when compared with the neighbouring Pannonian extensional basin. The basin architecture suggests that a deep lithospheric - asthenospheric mechanism is responsible for Middle - Late Miocene subsidence, coeval with phases of Carpathian collision. The interplay between upper crustal evolution and deep lithospheric mechanics is investigated by means of 2D lithospheric-scaled heat flow modelling, simulating the present-day thermal regime of the basin. The heat flow correction for transient effects shows the great importance of paleoclimate and sedimentation during the evolution of the basin, calculated values being ~20% higher when compared with measured heat flow. The modelling implies that the low values of heat flow are the result of a combination of thermal effects of Middle - Upper Miocene sedimentation and the presence of depleted rocks in the basin basement, with their thickness dependent on the amount of enrichment in felsic magmatism during their evolution in a supra-subduction zone. The observations infer a thinned lower part of the mantle during the Miocene evolution of the basin, but the lithosphere thermal time constant suggests such changes do not affect the thermal regime at present day. Larger effects in the SE part of the basin are likely driven by the recent asthenospheric uplift due to the Vrancea slab descent.

1. Introduction

The thermal structure of sedimentary basins and their evolution in time reflects the coupling between shallow crustal tectonics and deep lithosphere/upper mantle processes. In the absence of disturbing effects, the surface heat flow pattern is an important indicator of the lithospheric thermal state. The surface heat flow represents the sum of the amount of heat generated in the upper crust and transferred from the upper mantle. Fluctuations of the heat flow are driven by a large number of parameters, such as changes in crustal thickness, crustal heat production, deposition and/or erosion of sediments, climate variation, topography and variation of mantle heat flow (e.g., Blackwell et al.,

1980; Cermák, 1971; Hutchison, 1985; McKenzie, 1978; McKenzie et al., 2005; Powell et al., 1988). These parameters change the thermal characterization of sedimentary basins in terms of “cold” or “hot”, the reference being the average global values (continental crust around 55 mW/m², oceanic crust around 100 mW/m², e.g., Pollack et al., 1993, Stein, 1995, Turcotte and Schubert, 2002). When studying the thermal structure, the coupling between shallow tectonics and deep mantle processes can be investigated once all other parameters are understood. This is in particular relevant for sedimentary basins that do not contain upper crustal deformation structures, such as major fault systems that are genetically associated with their formation, commonly known as continental/interior sag, intra-cratonic sag or thermal sag basins (e.g.,

* Corresponding author at: Repsol Exploración S.A., Mendez Álvaro 44, 28045 Madrid, Spain.

E-mail address: marius.tilita@gmail.com (M. Tiliță).

<https://doi.org/10.1016/j.gloplacha.2018.07.007>

Received 31 May 2017; Received in revised form 3 May 2018; Accepted 13 July 2018

Available online 18 July 2018

0921-8181/ © 2018 Published by Elsevier B.V.

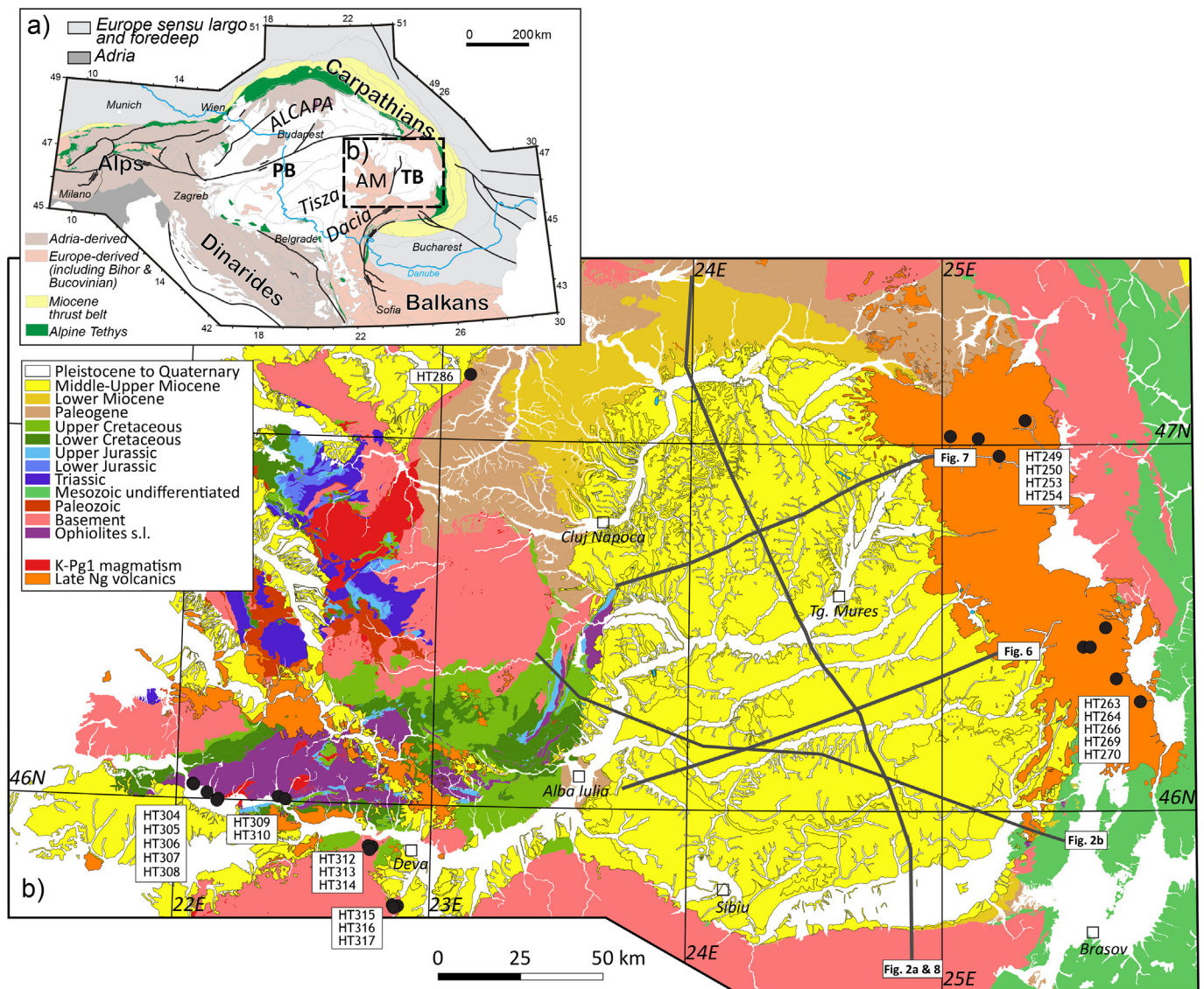


Fig. 1. Location of the Transylvanian Basin within the Alps-Carpathians-Dinarides system (simplified from Matenco and Radivojević, 2012; Schmid et al., 2008). b) Simplified geological map of Transylvanian Basin and surrounding orogens (modified after geological maps published by Institutul Geologic al Romaniei, scale 1:200,000) with the location of regional cross sections displayed in Fig. 2 and cross-sections used for the 2D thermal finite difference modelling Figs. 6, 7, 8. TB – Transylvanian Basin, PB – Pannonian Basin, AM – Apuseni Mountains.

Middleton, 1989; Ziegler et al., 2006). In such basins, understanding deep mantle processes associated with basin formation is facilitated by the means of thermal modelling, in particular when the geometry of sediments and the inherited crustal composition are known.

One common characteristic of Mediterranean arcs is the rapid evolution of extensional back-arc basins that formed at the interior of highly bended orogens in response to the roll-back of the genetic associated subduction zones (e.g., Faccenna et al., 2004; Jolivet and Faccenna, 2000). These continental or oceanic back-arc basins are dominated by major upper crustal extension, commonly associated with the rapid onset of a highly elevated thermal regime, as commonly observed in the Alboran Domain, Tyrrhenian Basin, Pannonian Basin or Aegean Sea (e.g., Jolivet and Brun, 2010; Horváth et al., 2006; Panza et al., 2007; Pepe et al., 2004; Vissers, 2012). When studying the thermal regime, one particularly contrasting area is the Transylvanian Basin, which was formed during the Middle-Late Miocene times in the hinterland of the Romanian Carpathians (Fig. 1, e.g., Krézsek and Bally, 2006; Tiliță et al., 2013). The Transylvanian Basin is in strong contrast in terms of tectonic evolution and thermal structure with the main

extensional back-arc basin of the intra-Carpathian area, i.e. the Pannonian Basin, which displays the typical characteristics of the Mediterranean back-arcs. The Pannonian Basin is associated with large-scale extension accommodated along lower-crust exhuming detachments that migrate in space and time across the basin (e.g., Matenco and Radivojević, 2012; Tari et al., 1999). It is also the hottest basin in continental Europe, underlined by highly thinned continental crust, the heat flow values reaching locally 120 mW/m^2 (e.g., Dövényi and Horváth, 1988; Lenkey et al., 2002).

Traditionally, the genesis of the Transylvanian Basin has been linked to different genetic processes ranging from extension to strike-slip deformation, slab roll-back, retro-foreland compression (e.g., Ciulavu et al., 2000; Horváth, 1993; Huismans and Bertotti, 2002; Royden et al., 1982; Royden, 1988; Sanders et al., 1999; Sclater et al., 1980). However, recent studies demonstrate minor extension in the Transylvanian Basin (Krézsek et al., 2010; Tiliță et al., 2013) with a rather contrasting thermal structure: a cold basin with average heat flow of 45 mW/m^2 that locally increases up to 110 mW/m^2 . The latter areas correspond to volcanic structures created by the Neogene

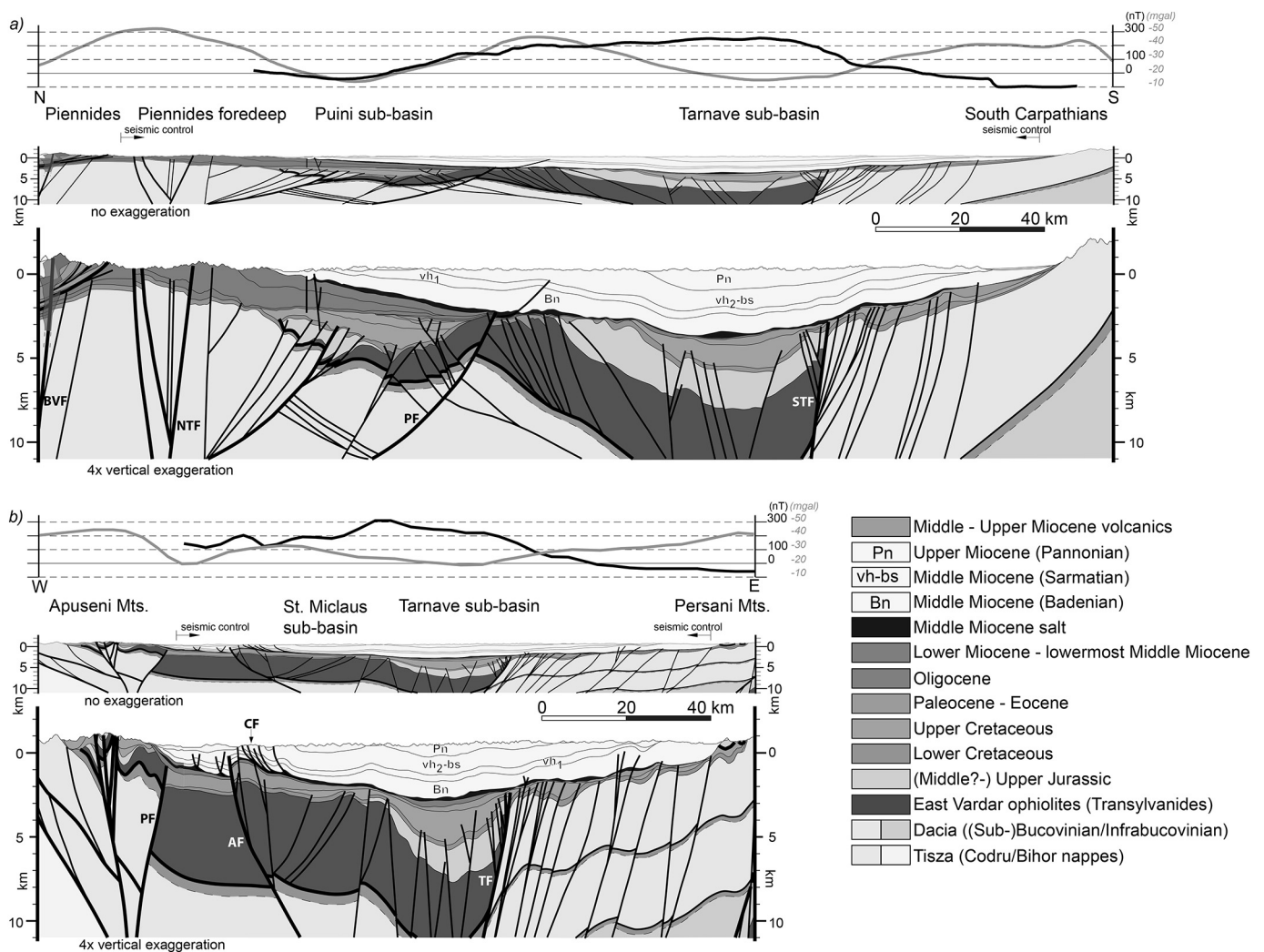


Fig. 2. Regional geological cross sections over the Transylvanian Basin derived from depth converted seismic interpretation extended over the basin margins (from Tiliță et al., 2013), together with gravimetric (Bouguer) and magnetometric (geomagnetic/aeromagnetic) profiles (after Besutiu et al., 2005). a) N–S cross-section over the Transylvanian Basin linking the ALCAPA unit in the north with the South Carpathians in the south (see Fig. 1b); b) E–W cross-section in the southern part of the Transylvanian Basin spanning from the Apuseni Mountains to the East Carpathians (see Fig. 1b). 1. BVF – Bogdan Vodă Fault; NTF – North Transylvanian Fault; STF – South Transylvanian Fault; TF – Târnave Fault; PF – Puini Fault; AF – Appulum Fault.

magmatism (Fig. 1, e.g., Demetrescu et al., 2001; Lenkey et al., 2002; Veliciu and Visarion, 1984). Outside the basin, the Carpathian orogen and its foreland shows heat flow values in the order of 50–80 mW/m² (e.g., Demetrescu et al., 2005; Lenkey, 1999). The more external Moesian and East European platforms displays low heat flow values of 40–50 mW/m² (e.g., Andreescu et al., 1989).

Existing studies of the thermal structure in the Transylvanian Basin explain the low surface heat flow as being the result of Middle-Upper Miocene rapid sedimentation and a strong depletion in heat producing elements or a small mantle heat influx (e.g., Andreescu et al., 2002; Cranganu and Deming, 1996; Demetrescu et al., 2001). The latter is in contrast with deep mantle geophysical and volcanological studies that infer an uplifted position of the asthenosphere beneath the basin (e.g., Ismail-Zadeh et al., 2012; Russo and Mocanu, 2009; Seghedi et al., 2011). Such contrasting inferences and the uniqueness of the Transylvanian Basin in the framework of the Mediterranean extensional back-arc systems are intriguing.

This study investigates the thermal state of the Transylvanian lithosphere and its relation with lithospheric-scale mechanics and basin formation by modelling the steady state temperature structure along 2D lithospheric-scaled sections. The study builds upon a recently improved geometry of the late Neogene basin (Tiliță et al., 2013), a better

understanding of lithology distribution inside the basin (Krézsek et al., 2010), recent heat flow measurements, updated petrophysical parameters (Andreescu et al., 2002; Demetrescu and Veliciu, 1991; Demetrescu et al., 2001; Serban et al., 2001a, 2001b) and advances of lithosphere-asthenosphere interactions in the hinterland of the Carpathians chain (e.g. Ismail-Zadeh et al., 2012). One of the study aims is to correct the present-day heat flow for the transient effects of past climate change and sedimentation/erosion in order to achieve a surface heat flow pattern reflecting only internal lithospheric processes. Another aim is to model the corrected heat flow pattern along sections assuming steady state thermal condition of the lithosphere. Finally, we draw conclusions about the thermal state of the lithosphere from the results of the modelling.

2. The evolution of the Carpathian hinterland

The Miocene evolution of the Carpathians was driven by the subduction roll-back of a slab situated at the exterior of the orogenic chain, that resulted from the closure of an oceanic embayment and its passive continental margin kinematically associated with the opening and evolution of the Alpine Tethys (e.g., Balla, 1986; Royden, 1988; Schmid et al., 2008). This slab was laterally attached to the cratonic units of the

Carpathians foreland - East European, Scythian and Moesian platforms, during Cretaceous to Miocene episodes of subduction and continental collision (Fig. 1, Matenco et al., 2010; Săndulescu, 1984). The roll-back was linked with the initiation of large scale back-arc extension in the Pannonian Basin, kinematically related with the extrusion of the Eastern Alps and translations accompanied with opposite sense rotations of the two main intra-Carpathians tectonic units, i.e. ALCAPA and Tisza – Dacia (Fig. 1, Csontos, 1995; Horváth et al., 2006; Ratschbacher et al., 1991; Schmid et al., 2013). The onset of extension in the Pannonian Basin was at ~20 Ma or possibly earlier during the Oligocene – Earliest Miocene and was accompanied by an overall migration of deformation in time and space across the basin throughout the remainder of Miocene times (Fodor et al., 1999; Horváth et al., 2006; Matenco and Radivojević, 2012; Toljić et al., 2013).

In this general framework, the Miocene evolution of the Transylvanian Basin, situated between the active subduction processes at the exterior of the Carpathians chain and the back-arc extension of the Pannonian Basin (Fig. 1), is superposed over an older Triassic – Eocene orogenic system.

2.1. The pre- Middle Miocene orogenic evolution of the Transylvanian Basin and its neighbouring areas

In the area of the East and South Carpathians, Apuseni Mountains and Transylvanian Basin, orogenic processes were initially derived from the Triassic–Jurassic opening of one other oceanic embayment, i.e. the Neotethys, and its subsequent closure by subduction and continental collision (e.g., Csontos and Vörös, 2004; Săndulescu, 1988; Schmid et al., 2008). Its northern European continental margin was affected by subsequent Jurassic rifting that was likely linked with the opening of the Alpine Tethys, which separated the Tisza block starting with Middle Jurassic times, coeval or shortly followed afterwards by the separation of the Dacia continental unit (e.g., Haas and Péró, 2004; Săndulescu, 1988; Schmid et al., 2008).

Subduction processes in the Neotethys Ocean ultimately lead to the Late Jurassic – Early Cretaceous emplacement by obduction and/or thrusting of large sheets of supra-subduction ophiolites over the metamorphic basement and Permian – Jurassic cover of the Dacia unit (Figs. 1–3). The obduction remnants are largely observed in the southern Apuseni Mountains, the basement of the Transylvanian Basin and as klippen overlying the basement and earlier sedimentary cover of the East Carpathians (Fig. 1, Hoeck et al., 2009; Ionescu et al., 2009; Schmid et al., 2008 and references therein). The latter phase of deformation was coeval with the creation of a thick-skinned nappe stack in the underlying continental Dacia unit (i.e. the Bucovinian and Getic nappes of the East and South Carpathians, Fig. 2) and by the initiation of subduction at the exterior of the East and South Carpathians (Iancu et al., 2005; Kräutner and Bindea, 2002; Săndulescu, 1988). The ophiolitic-bearing units outcropping in the Apuseni Mountains and intercepted in several boreholes across Transylvanian Basin also include Upper Jurassic island-arc, calc-alkaline volcanics and granitoidic intrusions (Fig. 3, e.g., Bortolotti et al., 2002, 2004; Ionescu et al., 2009; Pană et al., 2002; Saccani et al., 2001). All of these magmatics are stratigraphically sealed by Kimmeridgian-Neocomian thick shallow marine and platform carbonates and Lower Cretaceous marine clastics (e.g., Bleahu et al., 1981; Ciupagea et al., 1970; Săsăran, 2005).

This tectonic event was subsequently followed by Late Cretaceous extension, which created small basins in the Apuseni Mountains and larger offset normal faults buried at depth beneath the subsequent sedimentation of the Transylvanian Basin (e.g., the Târnave basin, Fig. 2, Krézsek and Bally, 2006; Schuller, 2004). The extension was interrupted by an intra-Turonian moment of large scale (back-)thrusting of the Dacia over Tisza units that created a thick-skinned nappe stack in the latter. This Tisza nappe stack is exposed in the Apuseni Mountains and mostly buried at depth in the Pannonian Basin (Fig. 2, Balintoni, 1996; Bleahu et al., 1981; Haas and Péró, 2004). The already sutured

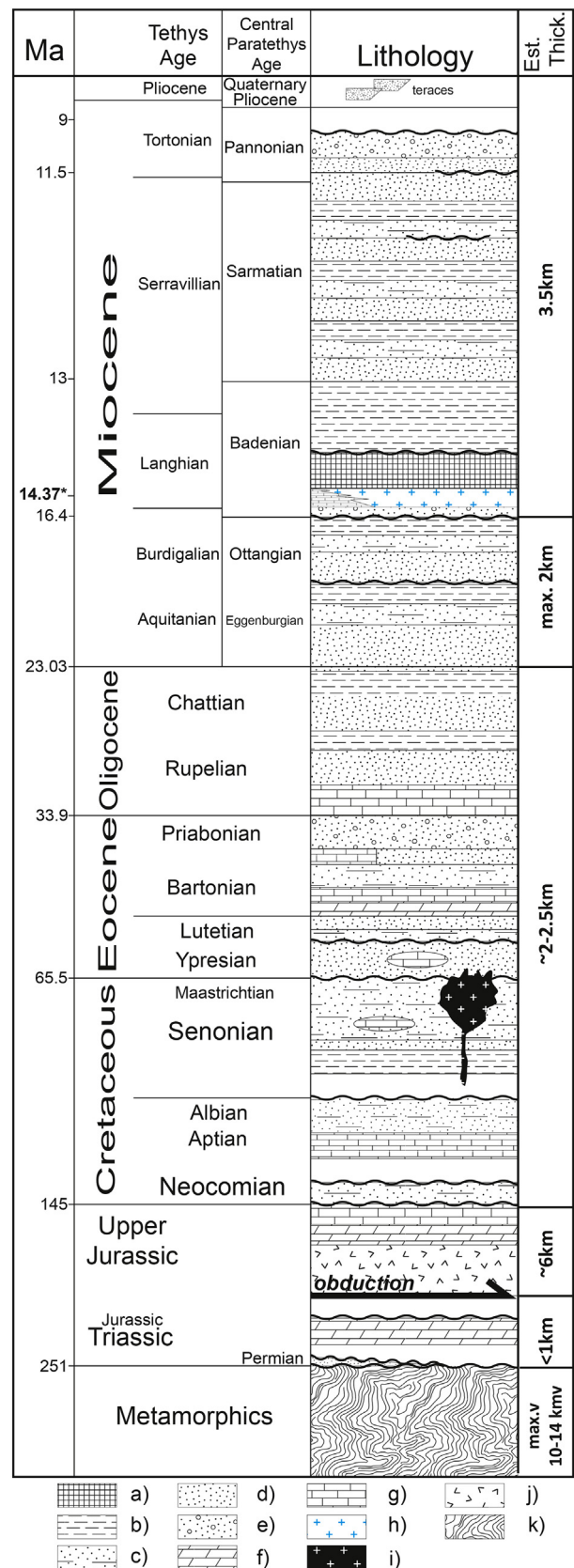


Fig. 3. Simplified stratigraphic column of the Transylvanian Basin (compiled from Ciupagea et al., 1970; De Broucker et al., 1998; Krézsek and Bally, 2006; Tiliță et al., 2013). a) salt, b) clays, c) marls, d) sandstones or sands, e) conglomerates, f) dolomites, g) limestones, h) tuff, i) K-Pg (Banatitic) magmatics, j) ophiolites, k) metamorphics. *) Dej Tuff age after de Leeuw et al., 2013.

Tisza-Dacia block was subsequently affected by thrusting during latest Cretaceous and Eocene times that created in the Transylvanian Basin low-offset thrusting cross-cutting the basement and locally inverting the late Cretaceous extensional basins (e.g., the Târnavă sub-basin, Fig. 2, see also Krézsek and Bally, 2006). This thrusting ultimately exhumed the Apuseni Mountains creating their dome-like structure (Merten et al., 2011) and emplaced the Ceahlău-Severin nappe creating the oceanic suture observed at the exterior of the East and South Carpathians (e.g., Săndulescu, 1988). The Upper Cretaceous sediments contain clastics, rudist limestones, shales and deeper marine turbidites (Fig. 3, e.g., Ciupagea et al., 1970; Krézsek and Bally, 2006). Lowermost Eocene deposits have a transgressive continental character in the Transylvanian Basin, followed by a mixture of shallow marine and continental sandstones, shelf carbonates or deep marine marls (Fig. 3). These sediments organized in several cycles are interpreted as an effect of successive periods of thrusting (e.g., Popescu, 1984; Proust and Hossu, 1996). During Oligocene clastic sedimentation continued with marls, bituminous shales, sandstones and conglomerates (Fig. 3).

At the end of Paleogene times, the basin was largely exhumed and significant amount of erosion is recorded until the onset of the subsequent Middle Miocene deposition (e.g., De Broucker et al., 1998; Paraschiv, 1997). The northern parts of the Transylvanian Basin recorded important subsidence during the latest Oligocene – Early Miocene times. These sediments are in fact a foredeep wedge tilted by the subsequent Miocene differential subsidence (Fig. 2a). This foredeep formed in response to the coeval thrusting of the ALCAPA block, an Adriatic derived unit, by northward shortening and eastward lateral escape into the basement of the Pannonian basin (Fig. 1), over the Tisza-Dacia unit (Csontos and Nagymarosy, 1998; Schmid et al., 2008; Tischler et al., 2008). The foredeep comprises a transition from shallow water clastics to deeper water turbidites and pelagic sedimentation (Fig. 3).

2.2. Middle–Upper Miocene subsidence and subsequent exhumation of the Transylvanian Basin

Shortening continued at the exterior of the East and South Carpathians during Oligocene – Miocene times, resulting in the formation of a wide thin-skinned thrust wedge, its exhumation culminating during the final 12–8 Ma moments of continental collision (e.g., Matenco et al., 2010; Merten et al., 2010). Partly coeval with the extension of the Pannonian Basin, the onset of subsidence in the Transylvanian Basin is recorded starting with the Middle Miocene times (Badenian, Fig. 3) and is associated locally with minor normal faulting with offsets reaching a couple of hundred metres (Krézsek et al., 2010). After the Early Badenian marine transgression, gradual basin deepening (Filipescu and Gîrbacea, 1997) and regional deposition of the rhyolitic Dej Tuff Complex (~14.4 Ma, de Leeuw et al., 2013, Seghedi and Szakács, 1991), a regional eustatic sea-level drop led to the deposition in average of 200–300 m thick evaporites, mostly salt (Fig. 3, e.g., de Leeuw et al., 2010; Tiliță et al., 2015). The subsidence continued with the deposition of almost 3.5 km of Upper Badenian – Pannonian sediments, typically fan-delta clastics organized in cycles driven by local tectonic or regional eustatic events (Fig. 3, Krézsek and Filipescu, 2005; Krézsek et al., 2010).

The final moments of Carpathians collision exhumed the basin towards the end of the Miocene period, which recorded only continental deposition (e.g., Matenco et al., 2010). This shortening is also illustrated in the basin by a reduced number of thrusts and folds with low offset truncating the pre-Miocene basement (e.g., the Appulum Fault -AF, Fig. 2, see also Tiliță et al., 2013). Starting with the end of Middle Miocene times, salt diapirism took place in the basin, normally recognized by low-amplitude pillow structures and folds in the overlying sedimentary sequence (Fig. 2). Large amounts of volcanic material was emplaced over the eastern margin of the Transylvanian Basin starting with the late Miocene and continuing until early Pliocene times, locally

exaggerating the underlying salt-diapirs (Seghedi et al., 2011; Szakács and Krézsek, 2006). The late Miocene shortening was followed by renewed moments of Quaternary out-of-sequence thrusting and large-scale exhumation restricted to the SE Carpathians that was genetically associated with subsidence in their foreland. This is generally interpreted as the result of a combined effect between on-going convergence and down-welling of the seismogenic active Vrancea slab, imaged by teleseismic mantle tomography (Ismail-Zadeh et al., 2012; Martin et al., 2006; Matenco et al., 2007; Merten et al., 2010).

2.3. Crustal, lithospheric and thermal structure in the large scale context

The crustal structure of the Transylvanian Basin has been investigated by a large number of studies focused in particular on the Vrancea seismogenic zone of the SE Carpathians. They include a recent combination of high-resolution methodologies, such as refraction and reflection seismics, and potential field geophysics (e.g., Bocin et al., 2013; Fillerup et al., 2010; Hauser et al., 2001; Hauser et al., 2007; Radulescu et al., 1976; Radulescu, 1988). These studies have demonstrated that the crust is 40–45 km thick beneath the Vrancea seismogenic zone and decreases beneath the basin, where it preserves around 35–37 km with a horizontal layering structure in the lower crust. The upper crustal composition and its expression in the magnetic and Bouguer gravity anomaly (Fig. 2) indicate a high compositional heterogeneity. The large magnetic anomaly corresponds to the thick ophiolites buried beneath the Târnavă sub-basin, while Bouguer anomaly isolates two areas of thick sedimentary stacks older than Middle-Upper Miocene, areas that overlap Târnavă and Puini sub-basins filled with Cretaceous sediments (see also Besutiu et al., 2005 and references therein).

The separation between upper and lower crust is less well understood, but refraction seismic along a NW-SE oriented profile suggest a rather constant upper crustal thickness in the order of 15 km partly in agreement with previous studies (Hauser et al., 2007; Radulescu, 1988). There is a discrepancy in the lithospheric thickness of the Transylvanian Basin highly dependent on the method of investigation. Studies based on seismology and magnetotellurics indicate thicknesses within 60–80 km (Fig. 4, e.g., Demetrescu and Veliciu, 1991; Horváth, 1993; Horváth et al., 2006; Stănică et al., 1986, 1999; Tari et al., 1999). Such interpretations show that the lithosphere is equally thinned beneath the Pannonian and Transylvanian Basin and, therefore, imply a common genetic mechanism. Alternatively, lithospheric modelling combining surface heat flow, geoid, gravity, and topography data infer much thicker lithosphere to values of around 100 km (Fig. 4, Dererova et al., 2006). Both studies indicate significant thickening beneath the East and Southeast Carpathians, and a gradual decrease towards the 60–80 km average lithospheric thickness of the Pannonian Basin. Teleseismic tomography, mantle attenuation, seismic anisotropy derived from SKS wave splitting and modelling studies suggest that the asthenospheric mantle is upwelling beneath the Transylvanian Basin, as part of a larger circuit that includes the downwelling of the Vrancea slab, as shown by high-velocity P-waves tomography (Fig. 4, e.g., Koulakov et al., 2010; Martin et al., 2006; Popa et al., 2005; Russo et al., 2005; Russo and Mocanu, 2009). Such an upwelling is also expressed by recent volcanism (Seghedi et al., 2011).

3. Geothermal modelling

The thermal state of the lithosphere is determined by tectonic events, mantle dynamics, near-surface processes and thermal parameters of constituent rocks. The peculiarity of the heat flow in the Transylvanian Basin is the extreme low value of 30 mW/m² in the middle of the basin (Fig. 5). Earlier thermal models of the Transylvanian Basin have inferred that the thermal imprint of Cretaceous tectonic events has largely decayed. The present-day near surface thermal field is influenced largely by the paleoclimatic surface temperature changes

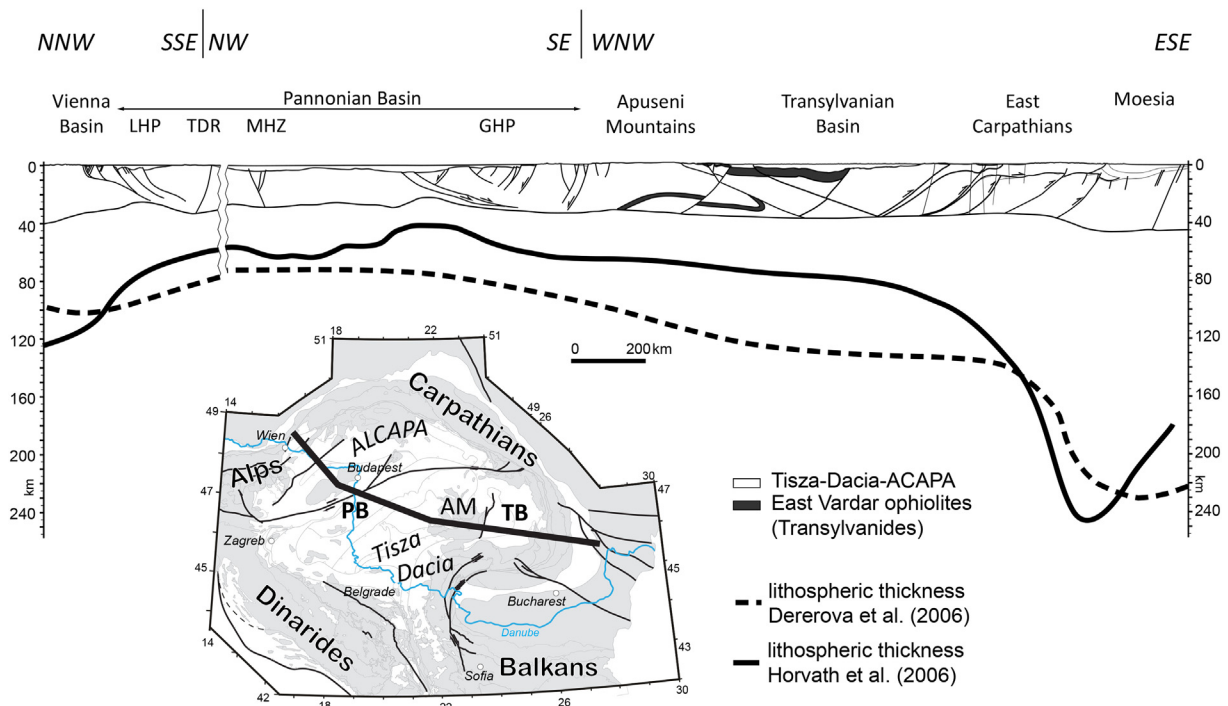


Fig. 4. Simplified regional cross-section showing the geometry of the intra-Carpathian lithospheric structure along a NW–ESE oriented transect crossing the Vienna and Pannonian basins, the Apuseni Mountains, the Transylvanian Basin and East Carpathians (from Tiliță et al., 2013). LHP — Little Hungarian Plain, TDR — Trans Danubian Range, MHZ — Mid Hungarian Zone, GHP — Great Hungarian Plain. Cross-section location displayed in inset showing Alps-Carpathians-Dinarides system (simplified from Matenco and Radivojević, 2012; Schmid et al., 2008).

and the Neogene sedimentation and erosion, while the role of topography and groundwater circulation can be ruled out (Andreescu et al., 2002; Demetrescu et al., 2001; Serban et al., 2001a). If the transient thermal effects of these processes are taken into account, the heat flow increases, but it remains below the mean continental value. Based on 2D temperature modelling Demetrescu et al. (2001) and Andreescu et al. (2002) explained the low heat flow by depletion in crustal heat production rate in the centre of the basin due to ophiolitic complexes obducted on the upper crust in this area.

The model covers the period from 23 Ma to present, since the genesis of actual basin began with a particularly sparse sedimentation in the Early Miocene (Krézsek and Filipescu, 2005; Tiliță et al., 2013) and ended with Late Miocene exhumation (Matenco et al., 2010), erosion becoming the only active process inside the basin. Therefore, the first step of the modelling consisted in correcting the present-day surface heat flow pattern for transient thermal effects of paleoclimate and sedimentation-erosion. This was performed by 1D modelling and was followed by 2D steady state modelling along three basin-wide cross-sections. The cross-sections were chosen in such a way to reflect in details the basin architecture and characteristics. The heat flow data, the control parameter of the modelling, are taken from two sources: Demetrescu and Velicic (1991), Demetrescu et al. (2001), Serban et al. (2001a, 2001b) and the International Heat Flow Commission (see Table 1, IHFC - Global Heat Flow Data Base section, <http://www.heatflow.und.edu/data.html>). The compilation of all these data has resulted in the heat flow map of the Transylvanian Basin and neighbouring areas (Fig. 5a). According to data distribution, the heat flow has good control in the centre of the basin where lies most of the measuring sites and less constrained along its flanks, which corresponds to less data. The exception is the eastern side of the basin, where the high values are the result of the late Miocene-Pliocene volcanic activity. In all other basin margin areas, the heat flow was estimated by interpolation with data adjacent to the basin. Similarly, to earlier studies (Andreescu et al., 2002; Demetrescu et al., 2001; Serban et al., 2001a), peripheral areas of the basin located outside the volcanic arc should be

characterized by a heat flow with average values for the Phanerozoic European continental crust of 60 mW/m^2 .

3.1. Transient thermal modelling

Long-term variations in surface temperature could significantly affect the temperature gradient down to 2 km leading to underestimation of the heat flow (e.g., Jaupart and Marechal, 2011; van Wees et al., 2009). The surface temperature increase at the end of the Weichselian glaciation ~12,000 years ago significantly affected the observed heat flow of the Transylvanian Basin (Serban et al., 2001a; Demetrescu et al., 2001). The latter publication presents a correlation between the depth and the magnitude of the paleoclimatic correction for the Transylvanian Basin, this correlation is applied again in this study for carrying out paleoclimatic correction to heat flow determinations uncorrected before (marked by RO):

$$\Delta q = -0.016 z_{max} + 21.2 \quad (1)$$

where Δq is the magnitude of the correction in mW/m^2 and z_{max} is the maximum depth of the heat flow determination in meters. Table 1 lists the wells used in this study, the uncorrected heat flow determined in them and the corrected values. The climate corrected surface heat flow (Fig. 5b) is similar to the one shown in Fig. 5a, but shifted upward by 5–15 mW/m^2 depending on the depth of the heat flow determination.

Other shallow processes in the Transylvanian Basin with influence on sub-surface temperature structure are the Late Neogene sedimentation and subsequent erosion. The evolution of temperature in the lithosphere due to sedimentation and erosion was calculated by solving the one-dimensional heat diffusion equation:

$$c\rho(z)\frac{DT}{Dt} = \frac{\partial}{\partial z} \left(k(z)\frac{\partial T}{\partial z} \right) + A(z) \quad (2)$$

where T is the temperature, t and z denote the time and depth respectively, and the material parameters: c , ρ , k and A are the specific heat, density, thermal conductivity and volumetric heat production

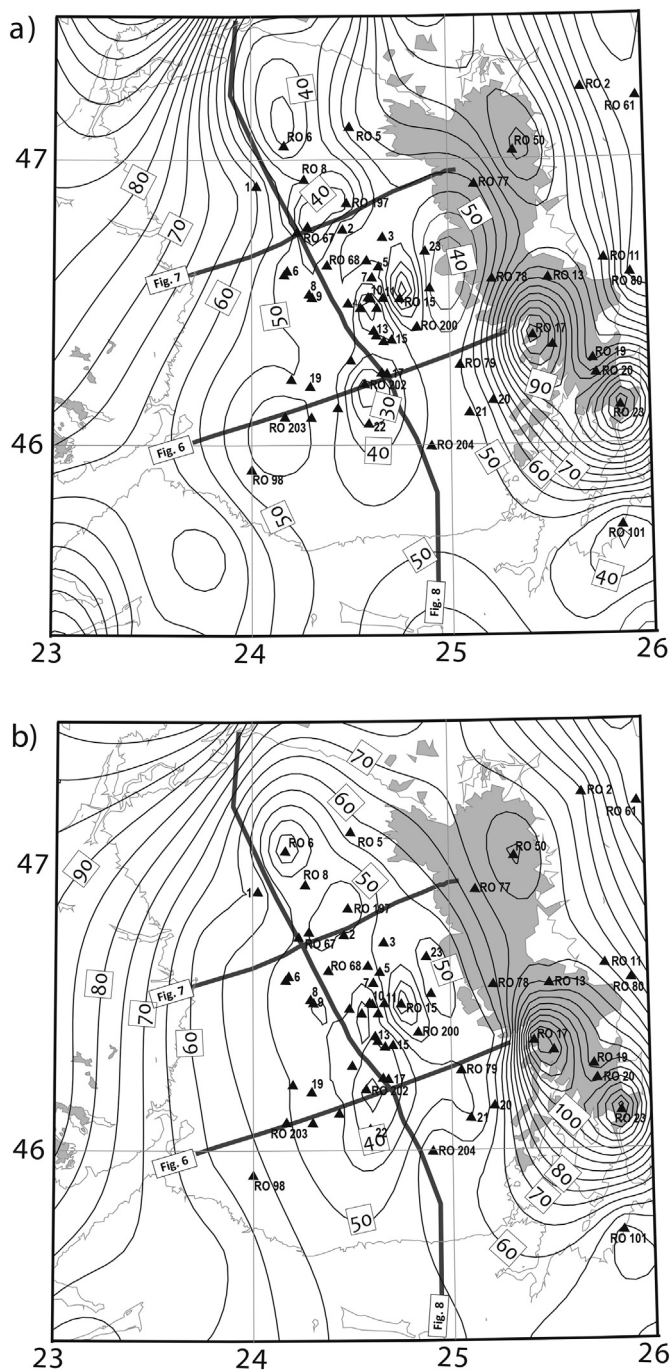


Fig. 5. a) Regional heat flow (uncorrected) map of Transylvanian Basin and surroundings, derived from borehole data published by [Hurtig et al. \(1991\)](#) and collected in the IHFC database (<http://www.heatflow.und.edu/data.html>, alphanumeric well codes), [Demetrescu et al. \(2001\)](#), [Demetrescu and Andrescu \(1994\)](#) and references therein (numerical well codes). See data in [Table 1](#). b) Regional heat flow map of the Transylvanian Basin and surrounding mountain chains corrected for paleoclimatic changes ([Table 1](#)). Overlaid are cross-section positions used in 2D thermal finite difference modelling ([Figs. 6–8](#)). For further details see the text.

rate. In Eq. (2), the material properties vary with depth due to compaction and lithology change ([Table 2](#)).

The solution was achieved using a finite difference method in a Lagrangian reference frame, where the nodes follow the material through the numerical grid ([Lucazeau and Le Douaran, 1985](#)). New nodes were added or removed at the top of the lithospheric column to

replicate sedimentation or respectively, erosion. The equation was solved using fully implicit method ([Press et al., 2007](#)). The assumed boundary conditions of the model were temperatures of 10 °C and 1300 °C at the surface and at the base of the lithosphere.

The initial condition of the transient model was the steady state temperature distribution in the lithosphere calculated using parameters from [Table 3](#) and boundary conditions given above. It resulted a steady state surface heatflow (Q_0) of 63 mW/m². Pre-requisite to solving Eq. (2) were decompaction of the sedimentary column, sedimentation rate for each layer derived from initial thickness and age of the layer and amount of eroded material in the late stage evolution. During simulation of deposition, values of the thermal parameters were re-calculated at every time step according to Eqs. (4)–(7). At the end of simulation, the present day sedimentary column was reached. Two parameters were introduced: the present day surface heat flow affected by sedimentation-erosion (Q_s) and the correction factor (R) as the ratio of the altered and steady state heat flows ($R = Q_s/Q_0$). In the last step, the corrected heat flow for sedimentation-erosion and paleoclimate was reached dividing paleoclimate corrected heat flow by R , operation repeated every 500 m along each cross-section. Further, the paleoclimatic correction was applied to the basin heat flow map ([Fig. 5a](#) and [b](#)) and punctually to wells positioned on or nearby model cross-sections ([Figs. 6–8](#)). The 1D approximation of basement tilting observed between the centre and the basin flanks shows 3% to 5%, resulting in < 5% error of the corrected heat flow.

3.2. Sedimentation and erosion history

Data provided by hydrocarbon exploration in Transylvania allowed the reconstruction of the accurate sedimentation history of the basin. Since the young deposition and erosion have the strongest effect on the heat flow, only the late Neogene formations have been considered in the transient thermal model. The deposition started during Lower Miocene (23 Ma) in the north ([Fig. 2a](#)) and continued in the entire basin during Middle-Late Miocene. A deposition rate of < 1 mm/yr can be derived assuming a compacted sediment thickness, while decompacted rates used in models increase close to 3 mm/yr. The Cretaceous and Paleogene sediments as shown by previous studies have a negligible effect on present day heat flow ([Andrescu et al., 2002](#); [Demetrescu et al., 2001](#)). The basin margins experienced limited erosion during short-lived moments of tectonic induced uplift in the neighbouring Carpathians, followed by the exhumation of the entire basin at the end of Miocene times ([Fig. 3](#), [Kręzek et al., 2010](#); [Matenco et al., 2010](#)). The amount of erosion was estimated to 4–7 km by earlier thermochronological studies on the neighbouring orogens (e.g., [Gröger et al., 2008](#); [Kounov and Schmid, 2013](#); [Merten et al., 2010](#); [Matenco et al., 2010](#); [Sanders et al., 1999](#); [Schuller, 2004](#)). Further, thermochronology derived erosion was correlated with the values derived from basin sequence stratigraphy inferring a linear decrease of cumulated amount of around ~1 km or ~0.14 mm/yr near the basin margins and around ~300 m or ~0.04 mm/yr in the centre of the basin ([Matenco et al., 2010](#)). The exception is the northern side of the basin, where the similar amounts of 5–7 km exhumation in the Rodna and Preluca Mountains ([Gröger et al., 2008](#)) took place at shorter distances from the basin, resulting in greater ~2 km or ~3 mm/yr amounts of erosion of the basin margin. In agreement with previous studies, the erosion in the model took place during Late Miocene – Quaternary times.

3.3. Steady state thermal modelling

After transient corrections applied to the surface heat flow pattern, the next step of the thermal modelling was to derive the surface heat flow delivered by steady state lithospheric-scale models populated with updated thermal parameters. There are two potential pathways in such types of thermal modelling, either to include well-known lithospheric kinematics and/or dynamics and set up transient models, or to assume

Table 1

Wells with heat flow determination used in this study. Wells 1–24 are taken after Demetrescu and Veliciu (1991), Demetrescu et al. (2001), Serban et al. (2001a, 2001b), wells marked by RO are taken after IHFC database (<http://www.heatflow.und.edu/data.html>). The paleoclimatic correction of Demetrescu et al. (2001) was used for the wells 1–24, while for the rest of wells was used Eq. (1) (see text). Paleoclimatic correction was performed only for those wells, where the depth of heat flow determination is given. Sedimentation correction was carried out only for wells located along the sections.

Site abbrev.	Well	Latitude (degrees)	Longitude (degrees)	Elevation (m)	Depth interval of heat flow determination (m)	Uncorrected heat flux (mW/m ²)	Heat flux corrected for paleoclimate (mW/m ²)	Heat flux corrected for paleoclimate and sedimentation (mW/m ²)
1	5 Puini	46.9100	24.0266	307	100–594	49	60	66
2	171 Craiesti	46.7580	24.4633	485	100–853	38	46	
3	13 Voivodeni	46.7320	24.6650	374	100–1217	50	54	
4	100 Ocnita	46.5000	24.4883	497	100–876	39	47	56
5	2 Dumbravioara	46.6280	24.6433	348	100–582	39	50	
6	195 Zau de Campie	46.6130	24.1817	362	100–1052	42	48	
7	10 Ernei	46.5900	24.6100	320	100–866	40	48	
8	17 Iclanzel	46.5320	24.2916	292	100–435	36	47	
9	196 Iclanzel	46.5200	24.3066	400	100–1316	42	44	
10	121 Tg Mures	46.5200	24.5900	414	100–751	31	41	
11	40 Corunca	46.5180	24.6650	387	100–506	36	47	
12	23 Tg Mures	46.5170	24.6033	356	100–861	34	42	
13	450 Filitelnic	46.4030	24.6166	316	100–1121	36	41	53
14	240 Filitelnic	46.3870	24.6300	379	100–1423	38	39	
15	161 Filitelnic	46.3720	24.7066	473	100–1266	36	39	
16	66 Filitelnic	46.3670	24.6666	367	100–739	32	42	
17	11 Prod	46.2570	24.6550	361	100–1047	31	37	46
18	110 Prod	46.2530	24.6816	408	100–1266	32	35	
19	39 Bazna	46.2080	24.2950	318	100–595	34	45	50
20	18 Beia	46.1580	25.2150	579	100–629	46	57	
21	13 Bunesti	46.1170	25.0950	589	100–1104	44	49	
22	143 Noul Sasesc	46.0780	24.5883	635	100–766	27	36	
23	1 Chiheru	46.6770	24.9831	580	100–980	40	46	
24	1 Nicolesti	46.4830	24.5500	400	100–980	29	35	44
RO 2	6-BRO	47.2510	25.6850	823	40–320	45	61	
RO 5	4135-BIS	47.1180	24.5011	400	1600–2600	58	58	
RO 6	4141-BEU	47.0520	24.1675	350	1400–2400	33	33	35
RO 8	16-FIN	46.9340	24.2683	374	80–980	45	50	
RO 11	281-BAL	46.6520	25.7842	1018	100–530	57	70	
RO 13	2-FIE	46.5860	25.5006	1250	120–270	77	94	
RO 14	1-MAG	46.5520	24.9014	500	80–980	39	45	
RO 15	F19	46.5170	24.7500	380	2050–2354	74	74	
RO 17	30-IVO	46.3850	25.4183	1048	120–520	113	126	
RO 18	2-VLA	46.3510	25.5178	950	30–220	104	122	
RO 19	33-SIN	46.3010	25.7183	1240	40–200	73	91	
RO 20	F18	46.2500	25.7333	525	314–510	83	96	
RO 23	1-H-TUS	46.1350	25.8517	600	20–540	118	131	
RO 50	ZEBRAC	47.0330	25.3333			82		
RO 61	CEAHLAU	47.2170	25.9667			36		
RO 67	SARMASEL	46.7500	24.2333			50		
RO 68	SINCAI	46.6330	24.3833			46		
RO 69	ZAU DE CIMPIE	46.6000	24.1667			48		
RO 70	HARANGLA	46.3000	24.5000			44		
RO 71	CETATEA DE BALTA	46.2330	24.2000			50		
RO 72	COPSA MICA	46.1000	24.3000			46		
RO 73	PAINGENU	46.6500	24.5833			50		
RO 76	NOUL SASESC	46.1330	24.4333			48		
RO 77	LUNCA BRADULUI	46.9170	25.1333			57		
RO 78	OCNA DE SUS	46.5830	25.2167			54		
RO 79	CRISTURU	46.2830	25.0500			50		
RO 80	VALEA REA	46.6000	25.9167			40		
RO 98	ALAMOR	45.9170	24.0000			46		
RO 101	TELIU	45.7170	25.8500			36		
RO 197	1-OCN	46.8510	24.4839	510	80–980	33	39	44
RO 198	10-SIL	46.7680	24.2856	475	80–500	30	43	49
RO 199	21-ACA	46.4830	24.6333	361	80–340	31	47	
RO 200	39-SIN	46.4170	24.8347	406	80–700	50	60	70
RO 202	1-DUM	46.2180	24.5692	353	80–940	26	32	39
RO 203	16-AXS	46.1010	24.1675	281	80–700	41	51	54
RO 204	10-BAR	46.0000	24.9017	579	80–440	46	60	65

steady state conditions. Because of the debated state and geometry of the lithosphere beneath the Transylvanian Basin (see discussion in Tiliță et al., 2013), the steady state thermal modelling approach was considered, the steady state conditions becoming the inferences for the

large-scale lithospheric evolution.

The temperature distribution in the lithosphere and the surface heat flow were modelled along the geological cross-sections by solving the 2D steady state heat conduction equation:

Table 2
Thermal parameters of the sediments (after Andreescu et al., 2002, Dövényi and Horváth, 1988) used in modelling the thermal effects of sedimentation.

	c (J/kg/K)	r (kg/m ³)	k (W/m/K)	Φ ₀ (%)	L (km)	A (μW/m ³)
Sand	800	2650	4.5	60	2.8	0.2
Clay	850	2600	2.8	70	2	1
Water	4186	1000	0.6			

$$0 = \frac{\partial}{\partial x} \left[k(x, z) \frac{\partial T}{\partial x} \right] + \frac{\partial}{\partial z} \left[k(x, z) \frac{\partial T}{\partial z} \right] + A(x, z) \quad (3)$$

Assumed boundary conditions are: no horizontal heat flow at the lateral margins and prescribed temperatures of 10 °C at the surface and 1300 °C at the bottom of the lithosphere (e.g., Turcotte and Schubert, 2002). The geometry of the model consists of three main layers: upper crust, lower crust and upper mantle. While the lower crust and the mantle were chosen of uniform compositions across the sections, the upper crustal structure and composition corresponded to the geometry imaged by seismic lines correlated with wells and crustal scale geophysics. In agreement with existing deep seismic reflection and refraction studies (Fillerup et al., 2010; Hauser et al., 2007), the upper crust was modelled as 15 km thick underlain by 21 km thick lower crust. The final model assumed a constant lithospheric thickness of 100 km beneath the basin (Dererova et al., 2006). The alternative thickness of 80 km (Horváth et al., 2006) had to be discarded since it would have resulted in a considerably higher heat flow. For example, similar conditions in the North East German Basin show a relatively high steady state heat flow of 77 mW/m² attributed to an attenuated lithosphere with thickness of 75 km (Norden et al., 2008). Reducing such a high heat flow to the values observed in the Transylvania basin with an 80 km thick lithosphere would require unreasonable material parameters and a thicker ophiolitic sequence in the basement of the basin.

Eq. (3) was solved through a finite difference method that used the successive over-relaxation algorithm -SOR (Press et al., 2007). The finite difference grid had equal 500 m horizontal spacing and vertically varying spacing of 100 m, 300 m and 1000 m in the upper crust, lower crust and mantle, respectively.

The solution shows the temperature distribution in the lithosphere.

Table 3
Thermal conductivity (k) and heat production (A) used in 2D modelling for the main upper crustal rock types, as well as for the sub-crustal section. Further descriptions and references in text.

	M-U Miocene	Bn2-salt	Pre-miocene	J3-carbonates	J-ophiolites	Metamorphics
W-E section (South – Fig. 6c)						
Thermal conductivity k (W/m/K)	1.5	1.5	2	3	3	3
Heat production A (μW/m ³)	0.5	0	0.5	0.4	m1-1 m2-0.15 m3-1.5	2
W-E section (North – Fig. 7c)						
Thermal conductivity k (W/m/K)	1.5	m1-1.5 m2-1.5 m3-6	m1-2 m2-3 m3-3	3	3	3
Heat production A (μW/m ³)	0.5	0	0.5	0.4	1	2
N-S section (Fig. 8c)						
Thermal conductivity k (W/m/K)	m1-1 m2-2 m3-1	1.5	2	3	3	3
Heat production A (μW/m ³)	0.5	0	0.5	0.4	m1-1 m2-1 m3-0.15	2
All sections						
		Upper crust		Lower crust		Mantle
Thermal conductivity k (W/m/K)		3.1		3.1		4
Heat production A (μW/m ³)		2		0.2		0

Further, this temperature was used to derive a new surface heat flow pattern, designated as the modelled heat flow. The variation of upper crustal thermal conductivities and heat production rates along cross-sections investigate their effect on the modelled heat flow. It also permitted to achieve a fit between the modelled and the corrected heat flows.

3.4. Material properties

A large part of thermal parameters are published data from papers that analysed in the past the thermal structure and evolution of the Transylvanian Basin (Andreescu et al., 2002; Demetrescu et al., 2001). The exception is the heat production rates of a few critical rocks present in the subsurface of the Transylvanian Basin, which were determined in this study by laboratory measurements of radioactive element concentration in rock samples (Table 4).

In the transient model (Eq. (2)), the thermal properties of sediments change with depth due to porosity decrease:

$$c_i \rho_i = c_w \rho_w \varphi_i(z) + c_{ip} \rho_{ip} (1 - \varphi_i(z)) \quad (4)$$

$$k_i(z) = k_w^{\varphi_i(z)} k_{ip}^{1-\varphi_i(z)} \quad (5)$$

$$A_i(z) = (1 - \varphi_i(z)) A_{ip} \quad (6)$$

$$\varphi_i(z) = \varphi_{0i} \exp\left(-\frac{z}{L_i}\right) \quad (7)$$

where φ is the porosity, L is the characteristic depth of the porosity decrease, index w refers to water and i refers to the type of sediment, in our case clay or sand, index p refers to the rock matrix and index 0 means surface value.

The Miocene sequence in the Transylvanian Basin is composed largely of siliciclastic sediments including clays, claystones, marly clays, sands, sandstones and conglomerates organized in parasequences, transgressive-regressive cycles and system tracts. This model considers only the fine and coarse fractions as clay and sand, respectively, their proportion being derived from existing sedimentological studies (Krézsek and Filipescu, 2005; Krézsek et al., 2010). These parameters were assumed constant throughout the basin for each given age: Lower Miocene 75% clay and 25% sand, Badenian 90% clay and

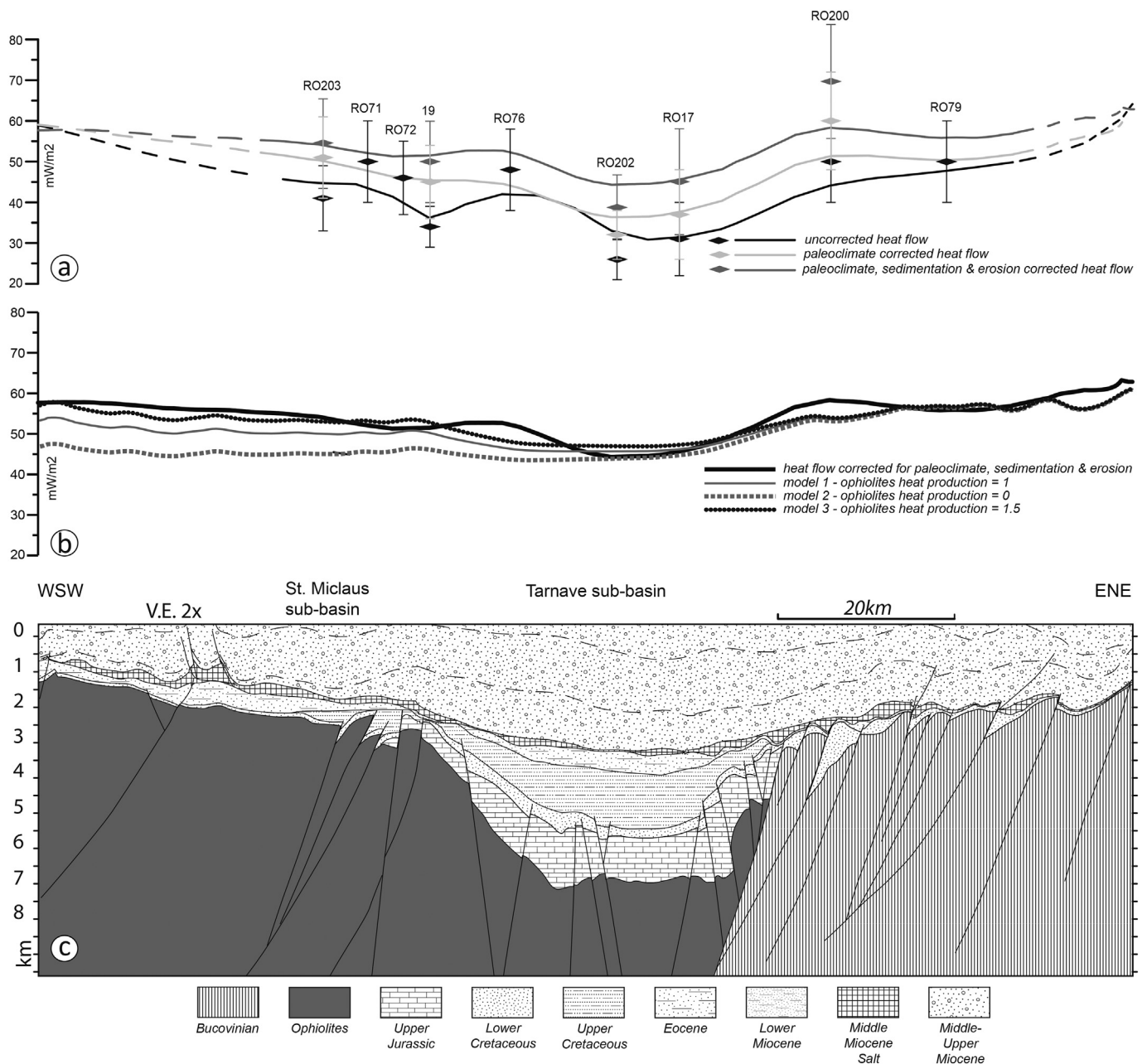


Fig. 6. Results of the 1D and 2D thermal modelling along a WSW-ENE oriented regional cross-section over the southern part of the Transylvanian Basin. Location in Figs. 1b and 5. a) Results of the 1D transient thermal modelling: uncorrected heat flow, correction for paleoclimate and additional correction for sedimentation/erosion. The uncorrected and paleoclimate corrected heat flow curves are taken from the heat flow maps presented in Fig. 5. Heat flow in wells located near the cross-section is also shown together with wells corrections. The error bar on the well data is $\pm 15\%$; b) Heat flow corrected for all transient effects and modelled heat flow curves along the section. 3 model results are superposed in the figure testing different scenarios of the ophiolites heat production; c) Geological cross-section along the selected transect (compiled from Krézsek and Bally, 2006; Matenco et al., 2010; Tiliță et al., 2013).

10% sand, Sarmatian 70% clay and 30% sand, Pannonian 70% clay and 30% sand. The average thermal conductivity of the mixed sediments was calculated as the weighted harmonic mean of the conductivities of clay and sand obtained from Eq. (5), where the weights are the proportions. Other thermal parameters of mixed sediments represent weighted averages of the parameters calculated in Eqs. (4) and (6). The salt was left out of the transient model and was replaced by Badenian sediments because at the time of deposition the salt was only 200–300 m thick (Krézsek and Bally, 2006; Tiliță et al., 2015). Such a small thickness does not influence significantly the transient heat flow (Andrescu et al., 2002). The properties of clays and sand (Table 2) are as suggested by Andrescu et al. (2002). This study chose to replace

their thermal conductivity of pure clay because such values would result in conductivities below 1 W/m/K. The new value used was the one determined for genetically related clays of the Pannonian Basin (Dövényi and Horváth, 1988) that yields more reasonable thermal conductivity values of around 1.5 W/m/K. This is in agreement with other values used for thermal modelling in the Transylvanian Basin (e.g., Demetrescu et al., 2001).

In the transient model, the upper crust beneath the interpreted cross-sections was considered as metamorphic rocks, in agreement with the deep structure of the Biharia and Bucovinian tectonic units that underlie ophiolitic nappes. The geometry and composition of the lower crust and upper mantle is the same in both transient and steady state

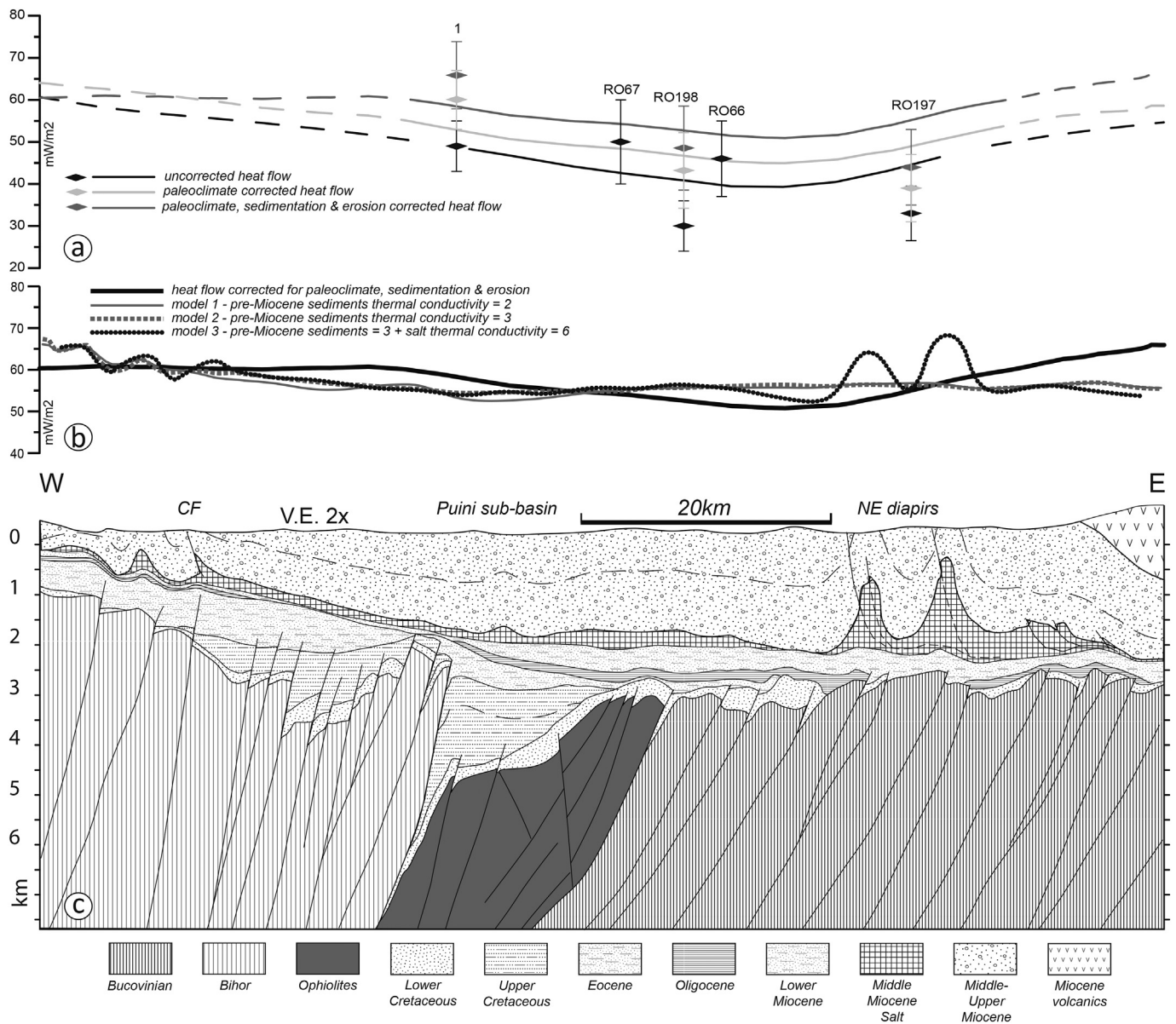


Fig. 7. Results of the 1D and 2D thermal modelling along a WSW-ENE oriented regional cross-section over the northern part of the Transylvanian Basin. Location in Fig. 1b and 5. a) Results of the 1D transient thermal modelling: uncorrected heat flow, correction for paleoclimate and additional correction for sedimentation/erosion. The uncorrected and paleoclimate corrected heat flow curves are taken from the heat flow maps presented in Fig. 5. Heat flow in wells located near the cross-section is also shown together with wells corrections. The error bar on the well data is $\pm 15\%$; b) Heat flow corrected for all transient effects and modelled heat flow curves along the section. 3 model results are superposed in the figure testing different values of thermal conductivity for the pre-Miocene sediments and salt; c) Geological cross-section along the selected transect (compiled from Krézsek and Bally, 2006; Matenco et al., 2010; Tiliță et al., 2013).

models.

In the steady state model (Eq. (3)), the values of thermal conductivity and heat-production rate for the Middle Miocene sediments were chosen as basin-wide averages (Table 3). Apparently a large amount of clay favours a low thermal conductivity value of 1.5 W/m/K, as high porosities relate to low heat production rates. Differently from the transient model, the salt was accounted in the steady state model, because its high conductivity (6 W/m/K) distorts the thermal field in places with thick diapirs, such as the large dome along the NE flank of the basin. The pre-Middle Miocene sediments (i.e. Triassic – Lower Miocene) were considered as a single siliciclastic unit, except the places where thick Upper Jurassic, Lower Cretaceous and Eocene carbonates are interpreted. The basement was modelled as a metamorphic sequence overlain by variable thickness ophiolites. Previous models (Matenco et al., 2010; Schmid et al., 2008) have assumed a distribution

of obducted ophiolites based on structural observation at their upper stratigraphic boundaries, but their thickness is little controlled. This study has preferred to assume in the initial structural model that the ophiolites have a larger thickness that spans until the base of the seismic investigation zone and the modelling tested this assumption. The part of the upper crustal section beneath this seismic investigation zone (i.e. until 15 km) was assumed to contain only metamorphic rocks. The lower crust and lithospheric mantle presume a mafic composition, i.e. depleted in heat production elements and with high thermal conductivities that range from 2.5 to 4.2 W/m/K (e.g., Jaupart and Marechal, 2011; Beardsmore and Cull, 2001 and references therein).

Since Jurassic ophiolites, island-arc volcanics, Neogene volcanics and metamorphic rocks are the main lithologic constituents of the investigated cross-sections, their heat production rate directly influences the surface heat flow pattern. In order to enhance the reliability of our

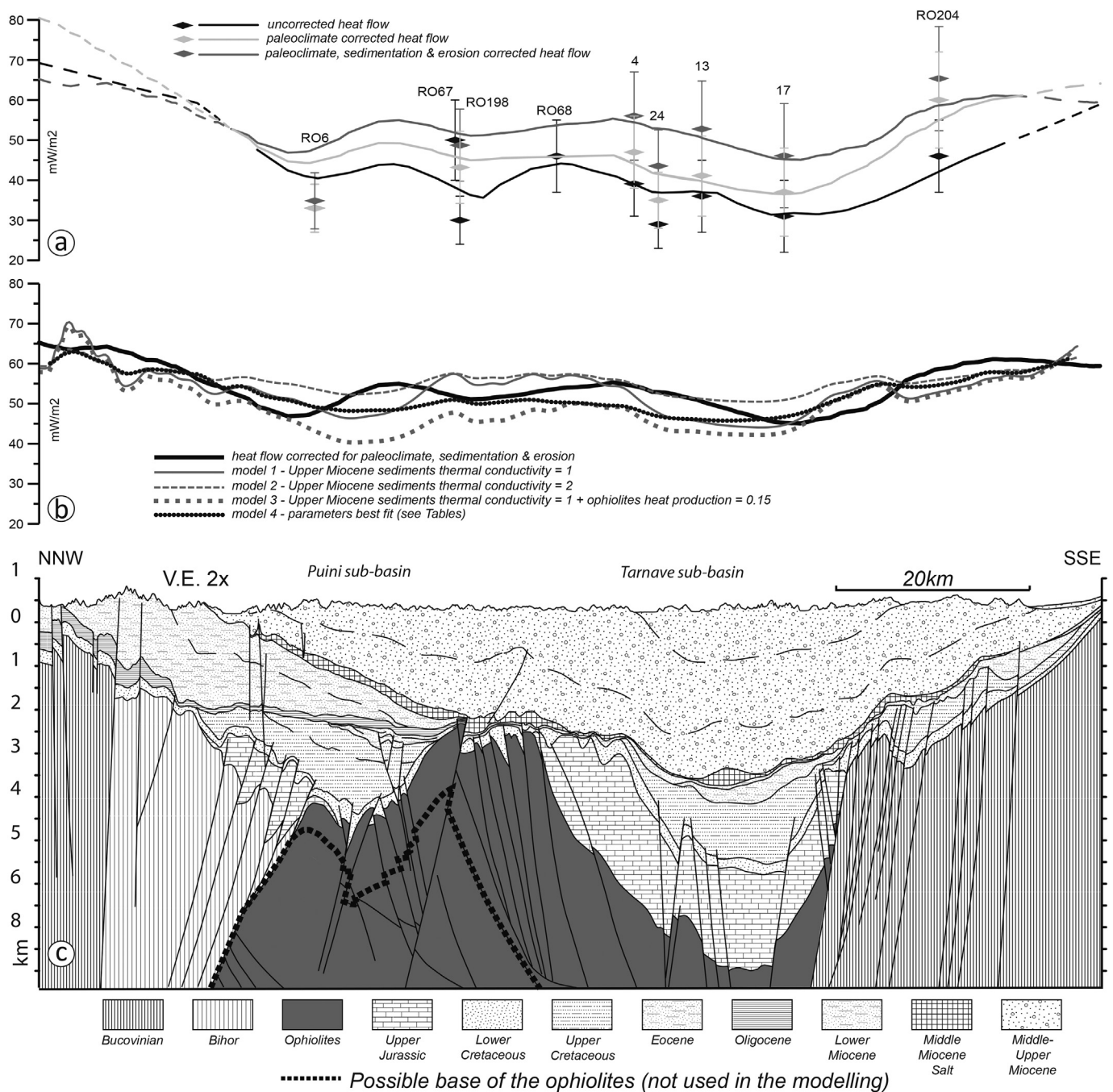


Fig. 8. Results of the 1D and 2D thermal modelling along a NNW-SSE oriented regional cross-section over the Transylvanian Basin. Location in Fig. 1b and 5. a) Results of the 1D transient thermal modelling: uncorrected heat flow, correction for paleoclimate and additional correction for sedimentation/erosion. The uncorrected and paleoclimate corrected heat flow curves are taken from the heat flow maps presented in Fig. 5. Heat flow in wells located near the cross-section is also shown together with wells corrections. The error bar on the well data is $\pm 15\%$; b) Heat flow corrected for all transient effects and modelled heat flow curves along the section. 4 model results are superposed in the figure together with best-fit scenario (see Tables 3 and 5 for details); c) Geological cross-section along the selected transect (compiled from Krézsek and Bally, 2006; Matenco et al., 2010; Tiliță et al., 2013).

model, several laboratory measurements were performed on outcrop samples for radioactive element concentrations - U, Th and K, allowing us to estimate the heat production rate. Collected samples are: andesites from the Neogene volcanics edifices, basalts from the laterally equivalent ophiolitic sequence of the southern Apuseni Mountains and low-degree metamorphic sequences of the Getic/Supragetic nappes of the South Carpathians. Sampling locations, rock types, radioactive element concentrations and heat production rates are synthesised in Fig. 1b and Table 4. U, Th and K concentrations were determined by gamma-ray spectrometry using shielded Canberra HPGe detector. We measured the

concentrations of intermediate isotopes in the decay series, rather than the parent U, Th and K. The conversion activity concentrations to elemental concentrations used the International Atomic Energy Agency (IAEA) standards of known concentrations, while Rybach's (1988) formula allows calculation of the heat production rate:

$$A = 10^{-5}\rho(9.51C_U + 2.56C_{Th} + 3.50C_K) \tag{8}$$

where A is the heat production rate in $\mu\text{W}/\text{m}^3$, C_U and C_{Th} are the concentrations of U and Th in ppm and C_K is the concentration of K in %.

The number and distribution of samples is generally insufficient to

Table 4

Measured heat production (A) from rocks belonging to units that constitute the basement of the Transylvanian Basin. Location of the sampling points is represented in Fig. 1. B(Oph) – basalt (ophiolite); M – metamorphics; A – andesite; Pz – Palaeozoic; LC – Lower Carboniferous; D/LC – Devonian – Lower Carboniferous.

Station	Latitude	Longitude	Rock	Th (ppm)	U (ppm)	K (%)	rho (g/cm ³)	A (μW/m ³)
HT304	46.0545	22.0489	B(Oph)	0.64	0.23	0.11	3.3	0.139
HT305	46.0545	22.0489	B(Oph)	0.37	0.13	0.20	3.3	0.095
HT306	46.0279	22.1218	B(Oph)	0.65	0.20	0.04	3.3	0.122
HT307	46.0034	22.1779	B(Oph)	1.29	0.42	0.03	3.3	0.244
HT308	45.9980	22.1715	B(Oph)	0.37	0.64	0.17	3.3	0.252
HT309	46.0191	22.4095	B(Oph)	0.43	0.30	0.10	3.3	0.142
HT310	46.0137	22.4374	B(Oph)	1.06	0.23	0.50	3.3	0.219
HT286	47.1761	23.1123	Pz-M	20.77	2.62	3.81	2.9	2.651
HT312	45.8810	22.7718	LC-M	12.75	3.06	1.78	2.9	1.971
HT313	45.8814	22.7707	LC-M	17.21	4.50	6.59	2.9	3.188
HT314	45.8806	22.7601	LC-M	8.08	1.89	2.04	2.9	1.328
HT315	45.7153	22.8857	LC-M	11.96	2.82	3.38	2.9	2.009
HT316	45.7138	22.8605	LC-M	21.76	4.26	1.66	2.9	2.959
HT317	45.7241	22.8494	D/LC-M	15.63	3.47	3.65	2.9	2.488
HT249	47.0066	25.0350	A	7.21	2.23	1.54	2.7	1.216
HT250	47.0103	25.1328	A	5.29	1.53	1.21	2.7	0.873
HT253	46.9679	25.1966	A	6.43	2.06	1.39	2.7	1.105
HT254	47.0504	25.3478	A	4.39	1.10	1.54	2.7	0.731
HT263	46.4530	25.5820	A	6.65	1.31	1.19	2.7	0.908
HT264	46.4525	25.5666	A	9.71	2.04	1.70	2.7	1.356
HT266	46.3633	25.6953	A	7.33	1.52	1.29	2.7	1.019
HT269	46.5040	25.6500	A	8.58	1.68	1.50	2.7	1.166
HT270	46.3006	25.7903	A	13.57	1.70	2.07	2.7	1.570
B(Oph) average				0.174				(μW/m ³)
M average				2.370				(μW/m ³)
A average				1.104				(μW/m ³)

derive statistical reliable distributions, in particular for the large variability of the metamorphic rocks in the Bucovinian/Getic/Biharia basement, but the values are comparable with the results of measurements for similar rocks elsewhere and, therefore, can be considered as most likely estimates for our modelling. For instance, concentrations in the basalts are in agreement with U, Th and K concentrations from Troodos ophiolites, Cyprus (Tzortzis and Tsertos, 2005) and ophiolitic meta-basalts from the Alps and Appenines (Chiozzi et al., 2002; Pasquale et al., 2001). Not surprisingly, the average U, Th and K concentrations in the Neogene andesites of the Transylvanian Basin are the same within the error margin with the ones of the Pannonian Basin (Lenkey and Surányi, 2006). A heat production rate of $2 \mu\text{W}/\text{m}^3$ was measured for metamorphic rocks, which is well within the range ($1\text{--}4.6 \mu\text{W}/\text{m}^3$) accepted for upper crustal rocks in lithospheric scale geothermal models (Kukkonen and Joeleht, 1996; Förster and Förster, 2000; Lewis et al., 2003).

4. Modelling results

The main scope of modelling is to evaluate at a higher resolution the thermal state of the Transylvanian crust and lithosphere, to evaluate effects derived from sedimentation/erosion processes, to investigate the effect of the spatial variation of the thermal conductivity and heat production due to lithologic variations and to speculate about the tectonic evolution of the basin.

4.1. Transient effects in the surface heat flow

The results indicate that the corrected heat flow is generally higher with values between 1 and $15 \text{ mW}/\text{m}^2$ and has a much more reliable distribution in the basin. The higher differences between the corrected and uncorrected heat flow values are observed in the centre of the basin where sediments are thickest, while differences decrease towards the basin margins proportional with the decrease in thickness (Figs. 6a, 7a and 8a). Notable is the dispersion among the values derived from heat

flow maps and well data, but the maps and profiles are always in the error range of well data (Figs. 5a, b, 6a, 7a and 8a). In addition to a yield in heat flow, the correction also smoothes its spatial distribution in profiles (Figs. 6a, 7a and 8a). This is only in part a result of correction, coming also from improving accuracy of the profiles by excluding those well data with missing reference depth, which further was hindering the paleoclimatic correction. It seems that such values have induced significant errors in the uncorrected version of the map(s) and profiles.

Modelling transient effects inferred that paleoclimatic changes and sedimentation/erosion processes have a significant effect in the present day distribution of heat flow (Figs. 5, 6a, 7a and 8a). The paleoclimatic correction accounts to an increase in the heat flow with values between 1 and $13 \text{ mW}/\text{m}^2$, with an average of $5\text{--}6 \text{ mW}/\text{m}^2$. The corrected heat flow map indicates minimum values in the central southern basin depocentre in the order of $40 \text{ mW}/\text{m}^2$ (Fig. 5b), despite the fact that southern part of the basin required the maximum correction (Fig. 8a). The low heat flow area is oriented NNW-SSE, following the overall structural trend of the basin. Outside this area, a local increase in heat flow to values above $60 \text{ mW}/\text{m}^2$ is observed in the central eastern part of the basin, while further eastwards values decrease to a normal $\sim 50 \text{ mW}/\text{m}^2$ for this structural flank. Two heat flow anomalies are observed locally in the SE part, overlapping Neogene volcanic structures with an age of $3\text{--}5 \text{ Ma}$. There is no obvious heat flow increase in relationship with older Miocene volcanic structures located more NWwards, but input data in this area is scarce (Fig. 5b). The heat flow minimum located in the central-southern part of the basin (Fig. 5b) overlaps with the area of highest Middle-Upper Miocene sedimentary thickness ($> 3.5 \text{ km}$) overlying the metamorphic and ophiolitic basement of the basin ($> 8 \text{ km}$). The paleoclimatic correction suggests $60\text{--}70 \text{ mW}/\text{m}^2$ and even higher heat flow values in the northern part over the basement margins (Fig. 8a), but these values decrease when applying the subsequent correction for erosion.

The correction for sedimentation increases the heat flow with additional values between 1 and $10 \text{ mW}/\text{m}^2$ (Figs. 6a, 7a and 8a).

Obviously, depending on sediment thickness, higher correction values are predicted for the centre of the basin where sediments are thickest, while these values decrease gradually towards the basin margins (Figs. 6a, 7a and 8a). The correction for erosion along the basin margins with exposed pre-Neogene cover and metamorphic/magmatic basement decreases the heat flow by up to 10 mW/m^2 (e.g., northern part of Fig. 8a). In general, these two corrections increased the heat flow minimum in the central-southern part of the basin to 45 mW/m^2 (Fig. 8a), while along the northern areas with maximum erosion rates heat flow reaches 55 mW/m^2 (Fig. 6a). Both values are below the average of continental crust in Europe (e.g., Cloetingh et al., 2010), but not significantly lower. For instance, similar heat flow values characterize the East-European craton at the exterior of the East Carpathians (Demetrescu et al., 2001). The model is more reliable inside the basin, where numerous thermal measurements are available and the reliability decreases towards or outside the basin margins, where such measurements are scarce.

4.2. 2D steady-state modelling of the surface heat flow

The 2D steady state model was applied along three cross-sections that were chosen to reflect contrasting styles of deformation and stratigraphic composition of pre-Miocene sediments and ophiolitic composition in the basement, while Middle-Upper Miocene sediments have similar geometries, but highly variable thicknesses.

The WSW-ENE oriented profile in the southern part of the Transylvanian Basin (Fig. 6c) shows the maximum growth of Middle – Upper Miocene sequence, thick Jurassic – Cretaceous sediments in the Târnavă sub-basin and ophiolites from the central and western parts of the basin. Further westwards, these ophiolites are laterally continuous over a late Cretaceous – Eocene thrust fault system with the ones largely exposed in the Southern Apuseni Mountains (see also Fig. 2b). Eastwards, the ophiolites are separated from the metamorphic Bucovinian unit and its Mesozoic cover by the large offset Late Cretaceous Târnavă Fault (TF), which was subsequently inverted during latest Cretaceous times (Fig. 6c). The model tested in particular the influence of the ophiolitic basement on the heat flow. Interestingly, the corrected heat flow does not correlate with the geometry of the ophiolites. It has a minimum over the Târnavă sub-basin, and it has a normal value of 60 mW/m^2 in the western part of the section, where ophiolites form the bulk of the basement. Therefore, it is no surprise that the modelled heat flow using the measured heat production rate of ophiolites ($0.15 \mu\text{W/m}^3$) misfits to the observed heat flow by up to 10 mW/m^2 . The best-fit curve was obtained with $1.5 \mu\text{W/m}^3$, which is one order of magnitude higher than the measured heat production value. This implies that either a thinner ophiolitic series is present in the basement or these ophiolites are not of normal MORB type, but contaminated with large amount of felsic material, i.e. with heat producing elements. The latter hypothesis is in agreement with the observation that these mafic rocks are not pure MORB, but oceanic island arc volcanics mixed with significant amounts of felsic intrusions (Ionescu et al., 2009). This composition was tested by modelling mixed heat production values between a basaltic composition and the felsic one of the island arc intrusions, assumed in our models to be similar to the one of the Neogene andesitic volcanics. This mixed composition (Table 5) resulted in a reasonably good fit, with slightly lower modelled heat flow values than the corrected ones.

The WSW-ENE oriented profile situated in the northern part of the Transylvanian Basin (Fig. 7c) contains the late Cretaceous – Eocene thrusting of the metamorphic Biharia unit and its Mesozoic – Paleocene cover over the ophiolites and their Late Jurassic – Cretaceous cover (i.e. the Puini thrust -PF), which are restricted to a narrower area in the centre of the profile. The latter are thrust during late Jurassic – Early Cretaceous times over the metamorphic Dacia (i.e. Bucovinian) unit and its Mesozoic cover. Smaller offset deformation is also observed locally in the profile, such as the late Cretaceous normal faulting in the

hanging-wall of the Puini thrust and latest Cretaceous thrusting in the Bucovinian basement. In this profile, large-scale salt-diapirism is observed locally exaggerated in the eastern part of the profile, where the thickness of the salt domes reaches 3 km. Salt diapirs with reduced thicknesses are also observed in the western part of the section (Fig. 7c). Therefore, in this profile the model tested, in particular, the influence of the salt diapirism and the influence of the thermal conductivity of pre-Miocene sediments. Two values were chosen for the thermal conductivity of the pre-Miocene sediments 2 and 3 W/m/K , while the third model tested the influence of salt by applying salt thermal conductivity of 6 W/m/K . Varying the thermal conductivity of pre – Miocene sediments does not have significant influence in the modelled heat flow. The model also shows that applying realistic salt thermal conductivity will increase the heat-flow with $10\text{--}12 \text{ mW/m}^2$ (Figs. 3–7b, c) above the 3 km thick salt domes. A similar effect, but with smaller amplitudes in the order of $5\text{--}7 \text{ mW/m}^2$ is also observed near the western border of the basin across the smaller salt diapirs. Elsewhere in the Transylvanian basin, where the salt has a tabular shape and lower thickness, varying its thermal conductivity shows negligible impact on heat flow.

The NNW-SSE oriented profile traversing along strike the entire Transylvanian Basin (Fig. 8c) displays a more complex structural style. Given the almost along strike orientation, the northern metamorphic basement of the Dacia unit is thrust over the ophiolites and their Upper Jurassic – Lower Cretaceous cover along a number of faults genetically related to the Puini thrust and is covered by the foredeep of this large thrust. Southwards, the ophiolites are separated from the Dacia metamorphic basement by the South Transylvanian Fault (STF) delimiting S-ward the Târnavă sub-basin, a late Cretaceous transtensional fault inverted by transpression during latest Cretaceous times. Between the Târnavă and Puini sub-basins, the ophiolitic basement is uplifted by latest Cretaceous – Eocene deformation, locally reactivated during Miocene times. In this profile, the model tested in particular the thermal refraction effect of the Middle – Upper Miocene sediments and the heat production of the ophiolites (Fig. 8b). The models demonstrate the importance of the heat refraction. In case of low thermal conductivity (1 W/m/K) the pattern of the modelled heat flow follows the topography of the basement; the heat flow is significantly reduced in the area of thick Miocene sediments and is increased where the high conductivity basement (ophiolites and Jurassic carbonates) is at shallower depths. As observed, high conductivities result in smoother and generally slightly higher heat flow. The best fit is achieved with sediment thermal conductivities of 1.5 W/m/K , which was also applied to the other profiles. The best fit confirms sediment parameters applied to the initial modelling setup (Table 2), parameters used to average the thermal conductivity of sediments across the profiles. Similarly to the south Transylvanian profile (Fig. 6b), applying the measured heat production rate of MORB basalts in the model underestimates the heat flow. A better fit was realised using higher heat production rates (Tables 4 and 5, Fig. 8b), which are consistent with depleted oceanic crust contaminated with felsic intrusions. Additionally, it is also possible that the thickness of ophiolites is less than assumed in Fig. 8c and resembling more a geometry depicted in Fig. 2.

However, none of the modelled curves using the initial input parameters was able to fit the observed and corrected heat flow values. To achieve the best fit (Fig. 8b), model parameters were adjusted within the limits provided by material properties (see Table 5) as follow: the mantle thermal conductivity was set to 3.2 W/m/K (a 0.8 W/m/K decrease), the lower crust thermal conductivity was set to 2.9 W/m/K (a 0.2 W/m/K decrease). The other thermal parameters were the same as the other models shown in Tables 3 and 4.

5. Discussion

The low values of heat flow in Transylvanian Basin can be reached with a combination of factors (e.g., Michaut et al., 2009; Perry et al., 2006), such as a strong crustal differentiation, unusually thick mantle

Table 5

Thermal conductivity (k) and heat production (A) parameters used to achieve a best-fit heat flow curve along the N–S cross-section (Fig. 9c). Further descriptions and references in text.

N–S section (Fig. 8c)	M-U Miocene	Bn2-salt	Pre-Miocene	J3-carbonates	J-ophiolites	Metamorphics
Thermal conductivity k (W/m/K)	1.5	1.5	3	3	3	3
Heat production A ($\mu\text{W}/\text{m}^3$)	0.5	0	0.5	0.4	1	2

N-S section (Fig. 8c)	Upper crust	Lower crust	Mantle
Thermal conductivity k (W/m/K)	2.9	2.9	3.2
Heat production A ($\mu\text{W}/\text{m}^3$)	2	0.1	0

lithosphere or large-scale structural control that creates a tectonic “melange” of components with high and low heat production values. Current geodynamic scenarios do not provide any reason to reduce the crustal heat production values or induce crustal differentiation of the basement beneath the Transylvanian Basin. The same type of crustal basement, either metamorphic or ophiolitic is observed laterally in areas where the heat flow is much higher (Carpathians, Apuseni Mountains, SW part of the Pannonian Basin, see the overviews of Matenco and Radivojević, 2012; Schmid et al., 2008). A significant increase in lithospheric thickness is conflicting with the results of high-resolution mantle velocity tomography or other geophysical studies (e.g., Ismail-Zadeh et al., 2012 and references therein).

The thermal modelling results indicate that the low heat flow in the Transylvanian Basin is a result of transient effects, lateral variation of the heat production controlled by the crustal structure and thermal refraction effect due to the low thermal conductivity of sediments.

5.1. Inferences of the 1D transient and 2D steady state modelling

Paleoclimate and sedimentation corrections increase the observed heat flow by 20% in the central area of the basin with thick Middle-Upper Miocene overburden. The corrected heat flow is $50 \text{ mW}/\text{m}^2$ in average across the basin, excluding localized anomalies overlying the volcanic centres (Fig. 6a). The magnitude of the correction depends on the rates of the sedimentation and the post-Late Miocene erosion. The model presented here assumes limited erosion (i.e., 300 m) in the central area of the basin. As erosion has the opposite effect to sedimentation, in another scenario with stronger erosion, the corrected heat flow values would be lower than in this study. In such a case, the low heat flow in the basin could be explained simply by the reduced heat production rate of ophiolites overlying the Bucovinian/Getic basement, a conclusion derived by previous studies (Andreescu et al., 2002; Demetrescu et al., 2001). However, a large amount of erosion inside the basin can be ruled out, because it would have increased the observed (uncorrected) heat flow (Table 1). We conclude that the proposed model uses a realistic scenario of deposition/erosion.

Interestingly, the model suggests that the average salt thickness in the Transylvanian Basin is too thin to induce significant changes in the heat flow distribution at the scale of the entire basin. In the NE part of the basin several large, but local, positive heat flow anomalies overprint a 2.5–3 km thick salt dome. When compared to other neighbouring salt diapirs with much lower amplitudes, this salt dome was overly exaggerated by rapid salt migration at high temperatures during the emplacement of the overlying volcanic sequences (i.e. volcanic sagging, Szakács and Krézsek, 2006). A similar increase in heat flow, but with lower amplitudes, is observed in the western part of the modelled section, due to salt diapirism in relationship with a regional shallow salt décollement (i.e. the Cenade Fault system) and its intersection with a basement involved thrust (i.e. the Appulum Fault, Figs. 2 and 3–8c, Ciulavu et al., 2000; Tiliță et al., 2013). All of these can be correlated with the North German Basin (Cacace et al., 2013) or the Pricaspian Basin (Ismail-Zadeh et al., 2010), where salt domes of several

kilometers thickness influence the heat flow with the same order of magnitude. Elsewhere in the basin, thin salt in range of 200–300 m does not appear to induce any significant effect on the modelled heat flow.

5.2. Large-scale structural control on the heat flow distribution in the basin

Our 2D thermal models infer that in order to match the modelled heat flow to the corrected one, a rather high value of heat production ($1\text{--}1.5 \mu\text{W}/\text{m}^3$) must be assumed for ophiolites (Tables 3 and 5, Figs. 6b and 8b). As stated earlier, such a value is rather improbable for typical MORB ophiolites and, therefore must reflect the observed combination with Jurassic island-arc volcanics and felsic intrusions.

Our assumption, that the ophiolites in the Transylvanian Basin are not (only) typical MORB's, is indeed in agreement with the observations of supra-subduction ophiolites, island-arc volcanics and felsic intrusions both in the Transylvanides nappes of the Southern Apuseni Mountains and East Carpathians (Bortolotti et al., 2002; Hoeck et al., 2009; Ionescu et al., 2009; Nicolae, 1994; Nicolae and Saccani, 2003), as well as their lateral continuation in the Eastern Vardar ophiolites (senso Schmid et al., 2008), of former Yugoslavia and Greece (e.g., Robertson et al., 2009). Furthermore, the ophiolites of the Apuseni Mountains contain latest Cretaceous – earliest Paleogene felsic Banatitic intrusions and volcanism and Neogene volcanics, stages of magmatism that were likely in the basement of the Transylvanian Basin (e.g., Berza et al., 1998; Krézsek and Bally, 2006; Seghedi et al., 2007; von Quadt et al., 2005). The large amounts of felsic intrusions would certainly increase the heat production of the ophiolitic unit, but a large distribution of felsic magmatism is not confirmed by exploratory wells and interpretation of the magnetic anomaly in the Transylvanian Basin (Besutiu et al., 2005; Ionescu et al., 2009).

The other possibility is that the thickness of the ophiolitic unit is less than the one proposed in our cross sections and is closer to the speculatively inferred one, by earlier interpretations (Schmid et al., 2008), i.e. note the different thickness of ophiolites in Fig. 2 when compared to Fig. 6c and 3–8c. This would imply that a greater thickness of metamorphic heat production crust is present beneath the ophiolites, which would resolve the discrepancy between the presence of ophiolites in the basement and the relatively high heat flow above them. Such an interpretation allows the occurrence of both MORB and supra-subduction ophiolites affected by island-arc volcanics and felsic intrusions, the difference being their overall thickness.

5.3. Inferences on the tectonics and evolution of the Transylvanian Basin from thermal modelling

After correcting for the near surface transient thermal processes, the heat flow in the Transylvanian Basin increases within the range of $45\text{--}55 \text{ mW}/\text{m}^2$. In the previous sections we have shown that this surface heat flow is consistent with a 100 km thick lithosphere in steady state. This interpretation is also in agreement with the pre-Miocene tectonic evolution of the basement. Following the Cretaceous - Eocene thick-skinned amalgamation of Tisza and Dacia units and the subsequent

shortening, the lithosphere of the Transylvanian Basin has reached thermal equilibrium. This normal lithospheric configuration is, however, in contrast with the thermal inferences derived from 3D numerical modelling of the lithosphere movement and mantle flow beneath the Vrancea region based on integrated analysis of seismic tomography, heat flow and gravity data (Ismail-Zadeh et al., 2005, 2008) That analysis infers ~80 km thick lithosphere beneath the basin, similar to the previously proposed configuration (Horváth, 1993 and Horváth et al., 2006). The discussion from Section 5.2 shows that the same surface heat flow can be achieved either by increasing the heat production rate of ophiolites or by reducing their thickness. As derived from potential theory, the same surface heat flow can be obtained with several combinations of thermal parameters. Thus, we could model the steady state surface heat flow of the Transylvanian basin in the case of 80 km lithospheric thickness too, applying the right thermal parameters. However, reduction of the lithospheric thickness leads to higher mantle heat flow and the low to medium surface heat flow of the basin would require a considerably reduced crustal heat production. This might be the case, especially because ophiolites are documented in the upper crust, even though their thickness is unknown. On the other hand, the scenario of high mantle heat flux combined with reduced crustal heat production in order to arrive at low to medium surface heat flow is quite specific. The authors do not rule out this possibility, but offer instead another theoretical scenario to explain the low to medium surface heat flow in case of 80 km lithospheric thickness: that the lithosphere of the Transylvanian basin is not in steady state.

The two processes influencing the “normal” lithospheric configuration in post-Paleogene times are the Middle Miocene subsidence coupled with the recent low-velocity anomaly acting in post-Miocene times beneath the SE Carpathians (Fig. 9), both mechanisms implying lithospheric mantle thinning at ~15 Ma and ~7 Ma, respectively. The lithospheric thinning mechanism was not stretching by pure shear deformation, because that would have led to an elevated heat flow into the crust. Therefore, the thinning process must have affected only the base of the lithosphere. The thermal time constant (τ) of the lithosphere

is estimated as follows:

$$\tau = L^2 / \kappa \pi^2 \tag{9}$$

where L is lithosphere thickness and κ is the thermal diffusivity. Given the thickness of the lithosphere (80–100 km) and the low value of thermal diffusivity ($10^{-6} \text{ m}^2/\text{s}$), the thermal time constant is higher (32 Ma) than the age of deformation (~20–16 Ma). Hence, the thermal effects of these processes do not have yet any near-surface expression and are still deep rooted in the lithosphere at ~70–80 km. Therefore, the near-surface temperature structure and the measured heat-flow still reflect the situation after the Cretaceous-Paleogene shortening and before any Miocene deformation.

The tectonic mechanism driving the regional Middle-Upper Miocene subsidence of the Transylvanian Basin must have been sub-crustal, because of the lack of significant Miocene structures at crustal scale and the lack of a positive thermal anomaly at the surface.

All recent deep geophysical passive and active studies have inferred a low-velocity anomaly localized beneath the SE Carpathians, in the immediate hinterland of the Vrancea slab, interpreted as the upwelling part of the asthenospheric circuit driven by the sinking of the slab (Fig. 9, Ismail-Zadeh et al., 2012; Koulakov et al., 2010; Martin et al., 2006 and references therein). This localized upwelling of the asthenosphere is associated with the formation of small Pliocene-Quaternary basins in the internal part of the SE Carpathians and adjacent Transylvanian Basin and with significant amounts of genetically related alkaline magmatism (e.g., Seghedi et al., 2011 and references therein). The large thermal anomalies observed locally in the southeast part of the Transylvanian Basin overlap with these volcanic centres (Fig. 5) and are part of the same late stage asthenospheric upwelling effect.

These Miocene to recent processes infer that the lithosphere of the Transylvanian Basin might have been actually much thicker at the end of the Cretaceous – Paleogene orogenic shortening and was ultimately reduced to the observed 80–100 km. This is in agreement with the observation that the Transylvanian Basin overlies a late Early Cretaceous suture zones formed in response to obduction, thrusting and continental

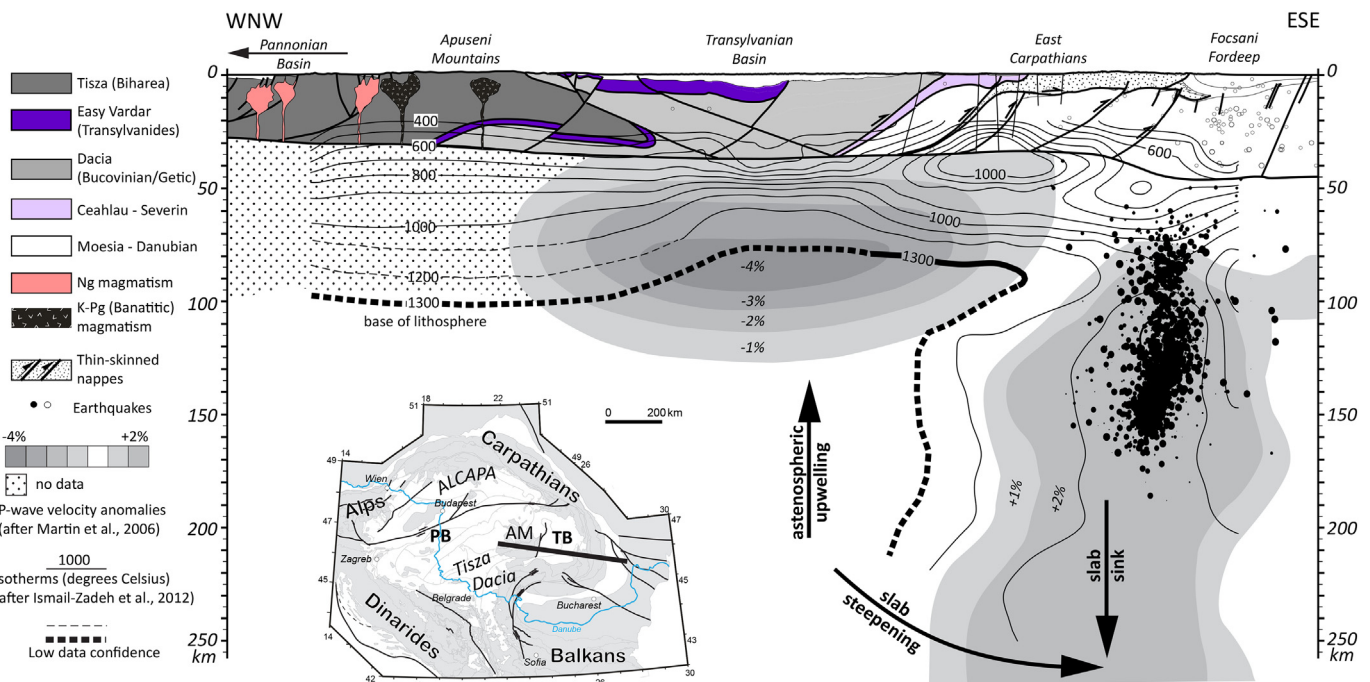


Fig. 9. Simplified cross-section showing the geometry and thermal structure of the lithosphere along a WNW–ESE oriented transect crossing the easternmost part of the Pannonian Basin, Apuseni Mountains, Transylvanian Basin and East Carpathians (from Matenco and Andriessen, 2013; Tiliță et al., 2013). Note that the perturbation of the isotherms in the upper mantle under Transylvania (isotherm configuration modified after Ismail-Zadeh et al., 2012) is a recent effect and is not considered by the steady-state modelling. Location displayed in inset showing Alps-Carpathians-Dinarides system (simplified from Matenco and Radivojević, 2012; Schmid et al., 2008). Further description in the text.

collision between Tisza and Dacia continental units.

6. Conclusions

Our analysis of the thermal structure of the sediments and their crustal and sub-crustal basement has the control of industrial data and surface observations combined with high resolution structural and sedimentological studies (e.g., Krézsek and Bally, 2006; Tiliță et al., 2013 and references therein). The 1D transient effects and 2D steady state modelling presented here have provided a number of key inferences for the tectonic evolution and basin development. The transient effects account for up to 20% increase in the surface heat flow pattern approaching the normal continental values, but with still low values when compared with the Pannonian Basin and locally in the Carpathians system. As the modelling suggests, these low values are the result of a combination between heat refraction of Middle–Upper Miocene overburden and the presence of ophiolites, island-arc volcanics and felsic intrusions in the basement of the basin. These ophiolites are the remnants of the East Vardar ocean obducted and/or thrust over its European margin during late Jurassic–Early Cretaceous times. The Middle Miocene salt is likely too thin to provide any significant differences in the heat flow pattern at the scale of whole basin, which are otherwise important in the case of the few locally exaggerated salt diapirs present along its eastern and western margin. The modelled heat flow was adjusted to the transient-corrected surface heat flow by varying the thermal conductivity and heat production of rocks. The best fit is obtained either assuming that the thick ophiolites have a normal upper crustal heat production rate, which contradicts measurements of heat production rates or assuming a reduced thickness of ophiolites to a few kilometers. This latter assumption is also in agreement with the nappe structure of the basement. The thickness of the ophiolitic unit is dependent on the compositional type and the variability of volcanics and intrusions, but cannot be thicker than ~7 km in the centre of the basin.

The exception to the normal steady state is observed in the SE part of our basin and is not constrained in our modelling study, since its recent effects are not yet observed in the near-surface thermal structure. It is likely that in this region the lithosphere has been recently thinned, starting in Pliocene times, by the upwelling part of the asthenospheric circuit driven by the sinking of the Vrancea slab (Fig. 9), as demonstrated by multiple geophysical studies (Ismail-Zadeh et al., 2012 and references therein). Similarly, the tectonic mechanism driving the regional Middle–Upper Miocene subsidence of the Transylvanian Basin does not have an imprint in the recent crustal thermal field due to the large time constant of the lithosphere. The actual thermal field of the basin corresponds to a 100 km thick lithosphere. It can be assumed that any Miocene back-arc extension and subsequent thinning of the lithosphere to 100 km, and later to 80 km, affected initially a thicker lithosphere (~120 km) derived from the late Cretaceous–Eocene shortening events. In both cases, the propagation of its effects has not affected yet the present upper crustal thermal expression.

Some of the latter hypotheses are still speculative at this stage of understanding the Pannonian – Carpathians lithosphere, but it demonstrates the need of continuing the analysis of the thermal structure combined with detailed crustal imagery and structural analysis such as the one presented in this study.

Acknowledgements

This publication is the result of a EUROBASIN Marie Curie Fellowship no. HPMT-GH-01-00306-07 and represents a collaboration between The Netherlands Research Centre for Integrated Solid Earth Science, Eötvös Loránd University of Budapest and University of Bucharest. Heat production rate measurements were supported by the Hungarian Science Fund - OTKA F034873. G. Bada and J.D. van Wees are gratefully thanked for their general support and suggestions. T. Harrold is acknowledged for his linguistic review.

References

- Andrescu, M., Burst, D., Demetrescu, C., Ene, M., Polonic, G., 1989. On the geothermal regime of the Moesian platform and Getic depression. *Tectonophysics* 164, 281–286.
- Andrescu, M., Nielsen, S.B., Polonic, G., Demetrescu, C., 2002. Thermal budget of the Transylvanian lithosphere. Reasons for a low surface heat-flux anomaly in a Neogene intra-Carpathian basin. *Geophys. J. Int.* 150, 494–505.
- Balintoni, I., 1996. Transilvanidele vestice, comentarii structurale. In: *Studia Universitatis Babeş-Bolyai Seria Geologia* XLI, pp. 95–100.
- Balla, Z., 1986. Palaeotectonic reconstruction of the central Alpine-Mediterranean belt for the Neogene. *Tectonophysics* 127, 213–243.
- Beardmore, G.R., Cull, J.P., 2001. *Crustal Heat Flow-A Guide to Measurement and Modelling*. Cambridge University Press (336 pp.).
- Berza, T., Constantinescu, E., Vlad, S.-N., 1998. Upper cretaceous magmatic series and associated mineralisation in the Carpathian - Balkan Orogen. *Resour. Geol.* 48, 291–306.
- Besutiu, L., Gorie, J., Dordea, D., Spranceana, V., 2005. Geophysical setting of the deep well 6042 Deleni in Central Transylvania-Romania. *Rev. Roum. Géophysique* 49, 73–84.
- Blackwell, D.D., Steele, J.L., Brott, C.A., 1980. The terrain effect on terrestrial heat flow. *J. Geophys. Res.* 85, 4757–4772.
- Bleahu, M., Lupu, M., Patrușiu, D., Bordea, S., Stefan, A., Panin, S., 1981. The Structure of the Apuseni Mountains. In: *Guide to Excursions B3, 12th Carpatho-Balkan Geological Association Congress*, Bucharest, Romania.
- Bocin, A., Stephenson, R., Matenco, L., Mocanu, V., 2013. Gravity and magnetic modelling in the Vrancea Zone, south-eastern Carpathians: redefinition of the edge of the East European Craton beneath the south-eastern Carpathians. *J. Geodyn.* 71, 52–64.
- Bortolotti, V., Marroni, M., Nicolae, I., Pandolfi, L., Principi, G., Saccani, E., 2002. Geodynamic implications of Jurassic ophiolites associated with island-arc Volcanics, south Apuseni Mountains, western Romania. *Int. Geol. Rev.* 44, 938–955.
- Bortolotti, V., Chiari, M., Maracussi, M., Marroni, M., Pandolfi, L., Principi, G., Saccani, E., 2004. Comparison among the albanian and greek ophiolites: in search of constraints for the evolution of the Mesozoic Tethys Ocean. *Ophioliti*, 29, 1–94.
- Cacace, M., Scheck-Wenderoth, M., Noack, V., Cherubini, Y., Schellschmidt, R., 2013. Modelling the surface heat flow distribution in the area of Brandenburg (northern Germany). *Energy Procedia* 40, 545–553.
- Cermák, V., 1971. Underground temperature and inferred climatic temperature of the past millennium. *Palaeogeogr. Palaeoclimatol. Palaeoecol.* 10, 1–19.
- Chiozzi, P., Pasquale, V., Verdoya, M., 2002. Naturally occurring radioactivity at the alps-Apennines transition. *Radiat. Meas.* 35, 147–154.
- Ciulavu, D., Dinu, C., Szakács, A., Dordea, D., 2000. Late Miocene to Pliocene kinematics of the Transylvania basin. *Am. Assoc. Pet. Geol. Bull.* 84, 1589–1615.
- Ciupagea, D., Pauca, M., Ichim, T., 1970. *Geologia bazinului Transilvaniei (in Romanian)*. Editura Tehnica, Bucuresti.
- Cloetingh, S., van Wees, J.D., Ziegler, P.A., Lenkey, L., Beekman, F., Tesauro, M., Förster, A., Norden, B., Kaban, M., Hardebol, N., Bonté, D., Genter, A., Guillou-Frotier, L., Ter Voorde, M., Sokoutis, D., Willingshofer, E., Cornu, T., Wörum, G., 2010. Lithosphere tectonics and thermo-mechanical properties: an integrated modelling approach for Enhanced Geothermal Systems exploration in Europe. *ci. Rev.* 102, 159–206.
- Cranganu, C., Deming, D., 1996. Heat flow and hydrocarbon generation in the Transylvanian Basin, Romania. *Am. Assoc. Pet. Geol. Bull.* 80, 1641–1653.
- Csontos, L., 1995. Tertiary tectonic evolution of the intra-Carpathian area: a review. *Acta Vulcanol.* 7, 1–13.
- Csontos, L., Nagymarosy, A., 1998. The mid-Hungarian line: a zone of repeated tectonic inversions. *Tectonophysics* 297, 51–71.
- Csontos, L., Vörös, A., 2004. Mesozoic plate tectonic reconstruction of the Carpathian region. *Palaeogeogr. Palaeoclimatol. Palaeoecol.* 210, 1–56.
- De Broucker, G., Mellin, A., Duindam, P., 1998. Tectono-stratigraphic evolution of the Transylvanian basin, pre-salt sequence, Romania. In: Dinu, C., Mocanu, V. (Eds.), *Geological structure and hydrocarbon potential of the Romanian areas*, Bucharest Geoscience Forum Special volume no. 1, Bucharest, pp. 36–69.
- de Leeuw, A., Bukowski, K., Krijgsman, W., Kuiper, K.F., 2010. Age of the Badenian salinity crisis; impact of Miocene climate variability on the Circum-Mediterranean region. *Geology* 38, 715–718.
- de Leeuw, A., Filipescu, S., Matenco, L., Krijgsman, W., Kuiper, K., Stoica, M., 2013. Paleomagnetic and chronostratigraphic constraints on the Middle to Late Miocene evolution of the Transylvanian Basin (Romania): implications for Central Paratethys stratigraphy and emplacement of the Tisza - Dacia plate. *Glob. Planet. Chang.* 103, 82–98.
- Demetrescu, C., Andrescu, M., 1994. On the thermal regime of some tectonic units in a continental collision environment in Romania. *Tectonophysics* 230, 265–276.
- Demetrescu, C., Veliciu, S., 1991. Heat flow and lithosphere structure in Romania. In: Cermák, V., Rybach, L. (Eds.), *Terrestrial Heat Flow and the Lithosphere Structure*. Springer-Verlag, Berlin, New York, pp. 187–205.
- Demetrescu, C., Nielsen, S.B., Enea, M., Șerban, D.Z., Polonic, G., Andrescu, M., Pop, A., Balling, N., 2001. Lithosphere thermal structure and evolution of the Transylvanian depression — insights from new geothermal measurements and modelling results. *Phys. Earth Planet. Inter.* 126, 249–267.
- Demetrescu, C., Wilhelm, H., Ene, M., Andrescu, M., Polonic, G., Baumann, C., Dobrica, V., Șerban, D.Z., 2005. On the geothermal regime of the foreland of the eastern Carpathians bend. *J. Geodyn.* 39, 29–59.
- Dererova, J., Zeyen, H., Bielik, M., Salman, K., 2006. Application of integrated geophysical modelling for determination of the continental lithospheric thermal structure in the Eastern Carpathians. *Tectonics* 25, TC3009. <https://doi.org/10.1029/2005TC001883>.

- Dövényi, P., Horváth, F., 1988. A review of temperature, thermal conductivity, and heat flow data for the Pannonian Basin. In: Royden, L.H., Horváth, F. (Eds.), *The Pannonian Basin, A Study in Basin Evolution*, pp. 195–233.
- Faccenna, C., Piromallo, C., Crespo-Blanc, A., Jolivet, L., Rosetti, F., 2004. Lateral slab deformation and the origin of the western Mediterranean arcs. *Tectonics* 23, TC1012. <https://doi.org/10.1029/2002TC001488>.
- Filipescu, S., Gîrbacea, R., 1997. Lower Badenian sea-level drop on the western border of the Transylvanian basin: foraminiferal paleobathymetry and stratigraphy. *Geol. Carpath.* 48, 325–334.
- Fillerup, M.A., Knapp, J.H., Knapp, C.C., Raileanu, V., 2010. Mantle earthquakes in the absence of subduction? Continental delamination in the Romanian Carpathians. *Lithosphere* 2, 333–340.
- Fodor, L., Csontos, L., Bada, G., Györfi, I., Benkovic, L., 1999. Tertiary tectonic evolution of the Pannonian basin system and neighbouring orogens: a new synthesis of paleostress data. In: Durand, B., Jolivet, L., Horváth, F., Seranne, M. (Eds.), *The Mediterranean Basins: Tertiary Extension within the Alpine Orogen*. The Geological Society, London, pp. 295–334.
- Förster, A., Förster, H.J., 2000. Crustal composition and mantle heat flow: implications from surface heat flow and radiogenic heat production in the Variscan Erzgebirge (Germany). *J. Geophys. Res.* 105, 27917–27938.
- Gröger, H.R., Fugenschuh, B., Tischler, M., Schmid, S.M., Foeken, J.P.T., 2008. Tertiary cooling and exhumation history in the Maramures area (internal eastern Carpathians, northern Romania): thermochronology and structural data. *Geol. Soc. Lond., Spec. Publ.* 298, 169–195.
- Haas, J., Péró, C., 2004. Mesozoic evolution of the Tisza mega-unit. *Int. J. Earth Sci.* 93, 297–313.
- Hauser, F., Raileanu, V., Fielitz, W., Bala, A., Prodehl, C., Polonic, G., Schulze, A., 2001. VRANCEA99—the crustal structure beneath the southeastern Carpathians and the Moesian platform from a seismic refraction profile in Romania. *Tectonophysics* 340, 233–256.
- Hauser, F., Raileanu, V., Fielitz, W., Dinu, C., Landes, M., Bala, A., Prodehl, C., 2007. Seismic crustal structure between the Transylvanian Basin and the Black Sea, Romania. *Tectonophysics* 430, 1–25.
- Hoeck, V., Ionescu, C., Balintoni, I., Koller, F., 2009. The Eastern Carpathians “ophiolites” (Romania): remnants of a Triassic Ocean. *Lithos* 108, 151–171.
- Horváth, F., 1993. Towards a mechanical model for the formation of the Pannonian basin. *Tectonophysics* 226, 333–357.
- Horváth, F., Bada, G., Szafian, P., Tari, G., Adam, A., Cloetingh, S., 2006. Formation and deformation of the Pannonian Basin: constraints from observational data. *Geological Society, London, Memoirs* 32, 191–206.
- Huismans, R., Bertotti, G., 2002. The Transylvanian basin, transfer zone between coeval extending and contracting regions: inferences on the relative importance of slab pull and rift push in arc-back arc systems. *Tectonics* 21, 1008. <https://doi.org/10.1029/2001TC900026>.
- Hurtig, E., Cermák, V., Haenel, R., Zui, V.I., 1991. *Geothermal Atlas of Europe*. Gotha Hermann Haack Verlagsgesellschaft (156 pp, 36 maps).
- Hutchison, I., 1985. The effects of sedimentation and compaction on oceanic heat flow. *Geophys. J. R. Astron. Soc.* 82, 439–459.
- Iancu, V., Berza, T., Seghedi, A., Gheuca, I., Hann, H.-P., 2005. Alpine polyphase tectonometamorphic evolution of the South Carpathians: a new overview. *Tectonophysics* 410, 337–365.
- Ionescu, C., Hoeck, V., Tomek, C., Koller, F., Balintoni, I., Besutiu, L., 2009. New insights into the basement of the Transylvanian depression (Romania). *Lithos* 108, 172–191.
- Ismail-Zadeh, A., Mueller, B., Schubert, G., 2005. Three-dimensional modeling of present-day tectonic stress beneath the earthquake-prone southeastern Carpathians based on integrated analysis of seismic, heat flow, and gravity observations. *Phys. Earth Planet. Inter.* 149, 81–98.
- Ismail-Zadeh, A., Schubert, G., Tsepeliev, I., Korotkii, A., 2008. Thermal evolution and geometry of the descending lithosphere beneath the SE-Carpathians: an insight from the past. *Earth Planet. Sci. Lett.* 273, 68–79.
- Ismail-Zadeh, A., Wilhelm, H., Volozh, Y., Tinakin, O., 2010. The astrakhan arch of the Pricaspian Basin: geothermal analysis and modelling. *Basin Res.* 22, 751–764.
- Ismail-Zadeh, A., Matenco, L., Radulian, M., Cloetingh, S., Panza, G., 2012. Geodynamics and intermediate-depth seismicity in Vrancea (the South-Eastern Carpathians): current state-of-the-art. *Tectonophysics* 530–531, 50–79.
- Jaupart, C., Marechal, J.-C., 2011. *Heat Generation and Transport in the Earth*. Cambridge University Press (476 pp).
- Jolivet, L., Brun, J.-P., 2010. Cenozoic geodynamic evolution of the Aegean. *Int. J. Earth Sci.* 99, 109–138.
- Jolivet, L., Faccenna, C., 2000. Mediterranean extension and the Africa-Eurasia collision. *Tectonics* 19, 1095–1106.
- Koulakov, I., Zaharia, B., Enescu, B., Radulian, M., Popa, M., Parolai, S., Zschau, J., 2010. Delamination or slab detachment beneath Vrancea? New arguments from local earthquake tomography. *Geochem. Geophys. Geosyst.* 11, Q03002.
- Kounov, A., Schmid, S., 2013. Fission-track constraints on the thermal and tectonic evolution of the Apuseni Mountains (Romania). *Int. J. Earth Sci.* 102, 207–233.
- Kräutner, H.G., Bindea, G., 2002. Structural units in the pre-Alpine basement of the Eastern Carpathians. *Geol. Carpath.* 53, 143–146.
- Krészek, C., Bally, A.W., 2006. The Transylvanian Basin (Romania) and its relation to the Carpathian fold and thrust belt: insights in gravitational salt tectonics. *Mar. Pet. Geol.* 23, 405–442.
- Krészek, C., Filipescu, S., 2005. Middle to late Miocene sequence stratigraphy of the Transylvanian Basin (Romania). *Tectonophysics* 410, 437–463.
- Krészek, C., Filipescu, S., Silye, L., Matenco, L., Doust, H., 2010. Miocene facies associations and sedimentary evolution of the southern Transylvanian Basin (Romania): implications for hydrocarbon exploration. *Mar. Pet. Geol.* 27, 191–214.
- Kukkonen, I.T., Joeleht, A., 1996. Geothermal modelling of the lithosphere in the Central Baltic shield and its southern slope. *Tectonophysics* 255, 25–45.
- Lenkey, L., 1999. Geothermics of the Pannonian Basin and its Bearing on the Tectonics of Basin Evolution. *Vrije Universiteit Amsterdam*, pp. 215.
- Lenkey, L., Surányi, G., 2006. A magyarországi neogén vulkánikus kőzetek hőtermelésének vizsgálata. (Heat production of Neogene volcanic rocks in Hungary. In Hungarian with English abstract). *Magyar Geofizika* 47 (4), 128–132.
- Lenkey, L., Dövényi, P., Horváth, F., Cloetingh, S., 2002. Geothermics of the Pannonian Basin and its bearing on the neotectonics. *European Geophysical Union Stephan Mueller Special Publications Series* 3, 29–40.
- Lewis, T.J., Hyndman, R.D., Flick, P., 2003. Heat flow, heat generation, and crustal temperature in the northern Canadian cordillera: thermal control of tectonics. *J. Geophys. Res.* 108 (B6), 2316.
- Lucazeau, F., Le Douaran, S., 1985. The blanketing effects of sediments in basins formed by extension: a numerical model. Applications to the Gulf of Lyon and Viking Graben. *Earth Planet. Sci. Lett.* 40, 92–102.
- Martin, M., Wenzel, F., The CALIXTO Group, 2006. High-resolution teleseismic body wave tomography beneath SE-Romania - II. Imaging of a slab detachment scenario. *Geophys. J. Int.* 164, 579–595.
- Matenco, L., Andriessen, P., 2013. From source to sink – quantifying the mass transfer from mountain ranges to sedimentary basins. *Glob. Planet. Chang.* 103, 1–18.
- Matenco, L., Radivojević, D., 2012. On the formation and evolution of the Pannonian Basin: constraints derived from the structure of the junction area between the Carpathians and Dinarides. *Tectonics* 31, TC6007. <https://doi.org/10.1029/2012tc003206>.
- Matenco, L., Bertotti, G., Leever, K., Cloetingh, S., Schmid, S., Tărăpoancă, M., Dinu, C., 2007. Large-scale deformation in a locked collisional boundary: interplay between subsidence and uplift, intraplate stress, and inherited lithospheric structure in the late stage of the SE Carpathians evolution. *Tectonics* 26, TC4011. <https://doi.org/10.1029/2006TC001951>.
- Matenco, L., Krészek, C., Merten, S., Schmid, S., Cloetingh, S., Andriessen, P., 2010. Characteristics of collisional orogens with low topographic build-up: an example from the Carpathians. *Terra Nova* 22, 155–165.
- McKenzie, D., 1978. Some remarks on the development of sedimentary basins. *Earth Planet. Sci. Lett.* 40, 25–32.
- McKenzie, D., Jackson, J., Priestley, K., 2005. Thermal structure of oceanic and continental lithosphere. *Earth Planet. Sci. Lett.* 233, 337–349.
- Merten, S., Matenco, L., Foeken, J.P.T., Andriessen, P.A.M., 2011. Toward understanding the post-collisional evolution of an orogen influenced by convergence at adjacent plate margins: Late Cretaceous–Tertiary thermotectonic history of the Apuseni Mountains. *Tectonics* 30. <https://doi.org/10.1029/2011TC002887>. (TC6008).
- Merten, S., Matenco, L., Foeken, J.P.T., Stuart, F.M., Andriessen, P.A.M., 2010. From nappe stacking to out-of-sequence postcollisional deformations: cretaceous to quaternary exhumation history of the SE Carpathians assessed by low-temperature thermochronology. *Tectonics* 29, TC3013.
- Michaut, C., Jaupart, C., Mareschal, J.-C., 2009. Thermal evolution of cratonic roots. *Lithos* 109, 47–60.
- Middleton, M.F., 1989. A model for the formation of intracratonic sag basins. *Geophys. J. Int.* 99, 665–676.
- Nicolae, I., 1994. Tectonic setting of the ophiolites from the South Apuseni mountains: magmatic arc and marginal basin. *Romanian Journal of Tectonics and Regional Geology* 76, 27–39.
- Nicolae, I., Saccani, E., 2003. Petrology and geochemistry of the Late Jurassic calc-alkaline series associated to Middle Jurassic ophiolites in the South Apuseni Mountains (Romania). *Schweiz. Mineral. Petrogr. Mitt.* 83, 81–96.
- Norden, B., Förster, A., Balling, N., 2008. Heat flow and lithospheric thermal regime of the northeast German Basin. *Tectonophysics* 460, 215–229.
- Pană, D.I., Heaman, L.M., Creaser, R.A., Erdmer, P., 2002. Pre-alpine crust in the Apuseni Mountains, Romania: insights from Sm-Nd and U-Pb data. *J. Geol.* 110, 341–354.
- Panza, G.F., Peccerillo, A., Aoudia, A., Farina, B., 2007. Geophysical and petrological modelling of the structure and composition of the crust and upper mantle in complex geodynamic settings: the Tyrrhenian Sea and surroundings. *Earth Sci. Rev.* 80, 1–46.
- Paraschiv, D., 1997. The pre-Paratethys buried denudational surface in Romanian territory. *Rev. Roum. Géogr.* 41, 21–32.
- Pasquale, V., Verdoya, M., Chiozzi, P., 2001. Radioactive heat generation and its thermal effects in the alps–Apennines boundary zone. *Tectonophysics* 331, 269–283.
- Pepe, F., Bertotti, G., Cloetingh, S., 2004. Tectono-stratigraphic modelling of the North Sicily continental margin (southern Tyrrhenian Sea). *Tectonophysics* 384, 257–273.
- Perry, H.K.C., Jaupart, C., Marechal, J.-C., Shapiro, N.M., 2006. Upper mantle velocity-temperature conversion and composition determined from seismic refraction and heat flow. *Journal of Geophysical Research – Solid Earth* 111 (B10), B07301.
- Pollack, H.N., Hurter, S.J., Johnson, J.R., 1993. Heat flow from the Earth's interior: analysis of the global data set. *Rev. Geophys.* 31, 267–280.
- Popa, M., Radulian, M., Grecu, B., Popescu, E., Placinta, A.O., 2005. Attenuation in Southeastern Carpathians area: result of upper mantle inhomogeneity. *Tectonophysics* 410, 235–249.
- Popescu, B.M., 1984. Lithostratigraphy of cyclic continental to marine Eocene deposits in NW Transylvania, Romania. 37. *Comptes Rendu des Seances, Societe de physique et d'histoire naturelle de Geneve*, pp. 37–73.
- Powell, W.G., Chapman, D.S., Balling, N., Beck, A.E., 1988. Continental heat flow density. In: Haenel, R., Rybach, L., Stegena, L. (Eds.), *Handbook of Terrestrial Heat Flow Density Determination*. Kluwer Academic Publishers, Dordrecht, pp. 167–222.
- Press, W.H., Teukolsky, S.A., Vetterling, W.T., Flannery, B.P., 2007. *Numerical Recipes: The Art of Scientific Computing*, 3rd edition. Cambridge University Press (1256 pp.).
- Proust, J.-N., Hosu, A., 1996. Sequence stratigraphy and paleogene tectonic evolution of the Transylvanian Basin (Romania, eastern Europe). *Sediment. Geol.* 105, 117–140.

- Radulescu, F., 1988. Seismic models of the crustal structure in Romania. *Rev. Roum. Géol. Géophys. Géogr., Sér. Géophys.* 32, 13–17.
- Radulescu, D.P., Cornea, I., Săndulescu, M., Constantinescu, P., Rădulescu, F., Pompilian, A., 1976. Structure de la crôte terrestre en Roumanie. *Essai d'interprétation des études séismiques profondes. An. Inst. Geol. Geofiz.* 50, 5–36.
- Ratschbacher, L., Frisch, W., Linzer, H.G., Merle, O., 1991. Lateral extrusion in the eastern alps; part 2, structural analysis. *Tectonics* 10, 257–271.
- Robertson, A., Karamata, S., Saric, K., 2009. Overview of ophiolites and related units in the late Palaeozoic-early Cenozoic magmatic and tectonic development of Tethys in the northern part of the Balkan region. *Lithos* 108, 1–36.
- Royden, L.H., 1988. Late Cenozoic tectonics of the Pannonian Basin system. *AAPG Mem.* 45, 27–48.
- Royden, L., Horváth, F., Burchfiel, B.C., 1982. Transform faulting, extension, and subduction in the Carpathian Pannonian region. *Geol. Soc. Am. Bull.* 93, 717–725.
- Russo, R.M., Mocanu, V.I., 2009. Source-side shear wave splitting and upper mantle flow in the Romanian Carpathians and surroundings. *Earth Planet. Sci. Lett.* 287, 205–216.
- Russo, R.M., Mocanu, V., Radulian, M., Popa, M., Bonjer, K.-P., 2005. Seismic attenuation in the Carpathian bend zone and surroundings. *Earth Planet. Sci. Lett.* 237, 695–709.
- Rybach, L., 1988. Determination of the heat production rate. In: Haenel, R., Rybach, L., Stegena, L. (Eds.), *Handbook of Terrestrial Heat-Flow Density Determination*. Kluwer Academic Publishers, Dordrecht, pp. 125–142.
- Saccani, E., Nicolae, I., Tassinari, R., 2001. Tectono-magmatic setting of the Jurassic ophiolites from the South Apuseni Mountains (Romania): petrological and geochemical evidence. *Ofioliti* 26, 9–22.
- Sanders, C., Andriessen, P., Cloetingh, S., 1999. Life cycle of the East Carpathian Orogen: erosion history of a doubly vergent critical wedge assessed by fission track thermochronology. *J. Geophys. Res.* 104, 95–112.
- Săndulescu, M., 1984. *Geotectonica României* (translated title: *Geotectonics of Romania*). Ed. Tehnică, Bucharest.
- Săndulescu, M., 1988. Cenozoic tectonic history of the Carpathians. In: Royden, L.H., Horváth, F. (Eds.), *The Pannonian Basin, a Study in Basin Evolution*. American Association of Petroleum Geologists Memoir Vol. 45, pp. 17–25.
- Săsăran, E.F., 2005. Upper Jurassic - Lower Cretaceous Carbonates Sedimentation from Bedeleu Nappe (Apuseni Mountains): Facies, Biostratigraphy and Sedimentary Evolution. *Facultatea de Biologie și Geologie. Babes-Bolyai University of Cluj Napoca, Cluj Napoca*, pp. 317.
- Schmid, S., Bernoulli, D., Fügenschuh, B., Matenco, L., Schefer, S., Schuster, R., Tischler, M., Ustaszewski, K., 2008. The Alpine-Carpathian-Dinaridic orogenic system: correlation and evolution of tectonic units. *Swiss J. Geosci.* 101, 139–183.
- Schmid, S., Scharf, A., Handy, M., Rosenberg, C., 2013. The Tauern window (Eastern Alps, Austria): a new tectonic map, with cross-sections and a tectonometamorphic synthesis. *Swiss J. Geosci.* 106, 1–32.
- Schuller, V., 2004. Evolution and geodynamic significance of the Upper Cretaceous Gosau basin in the Apuseni Mountains, Romania. *Universität Tübingen, Institut für Geowissenschaften, Tübingen*, pp. 112 (PhD thesis).
- Sclater, J.G., Jaupart, C., Galson, D., 1980. The heat flow through oceanic and continental crust and the heat loss of the Earth. *Rev. Geophys. Space Phys.* 18, 269–311.
- Seghedi, I., Szakács, A., 1991. The Dej tuff from Dej-Ciceu area: some petrographical, petrochemical and volcanological aspects. In: Bedeleu, I., Ghergari, L., Marza, I., Meszaros, N., Nicorici, E., Petrescu, I. (Eds.), *The Volcanic Tuffs from the Transylvanian Basin, Romania*. University of Cluj Napoca, Cluj Napoca, pp. 135–146.
- Seghedi, I., Bojar, A.-V., Downes, H., Rosu, E., Tonarini, S., Mason, P., 2007. Generation of normal and adakite-like calc-alkaline magmas in a non-subductional environment: an Sr-O-H isotopic study of the Apuseni Mountains neogene magmatic province, Romania. *Chem. Geol.* 245, 70–88.
- Seghedi, I., Matenco, L., Downes, H., Mason, P.R.D., Szakács, A., Pécskay, Z., 2011. Tectonic significance of changes in post-subduction Pliocene-Quaternary magmatism in the south east part of the Carpathian-Pannonian Region. *Tectonophysics* 502, 146–157.
- Serban, D.Z., Nielsen, S.B., Demetrescu, C., 2001a. Transylvanian heat flow in the presence of topography, paleoclimate and groundwater flow. *Tectonophysics* 335, 331–344.
- Serban, D.Z., Nielsen, S.B., Demetrescu, C., 2001b. Long wavelength ground surface temperature history from continuous temperature logs in the Transylvanian Basin. *Glob. Planet. Chang.* 29, 201–217.
- Stănică, D., Stănică, M., Visarion, M., 1986. The structure of the crust and upper mantle in Romania as deduced from magnetotelluric data. *Rev. Roum. Geol.* 30, 25–35.
- Stănică, M., Stănică, D., Marin-Furnica, C., 1999. The placement of the Trans-European Suture Zone on the Romanian territory by electromagnetic arguments. *Earth Planets Space* 51, 1073–1078.
- Stein, C.A., 1995. Heat flow of the Earth. In: Ahrens, T.J. (Ed.), *Global Earth Physics: A Handbook of Physical Constants*. AGU, pp. 144–158.
- Szakács, A., Krézsek, C., 2006. Volcano-basement interaction in the Eastern Carpathians: explaining unusual tectonic features in the Eastern Transylvanian Basin, Romania. *J. Volcanol. Geotherm. Res.* 158, 6–20.
- Tari, G., Dövényi, P., Dunkl, I., Horváth, F., Lenkey, L., Stefanescu, M., Szafian, P., Toth, T., 1999. Lithospheric structure of the Pannonian basin derived from seismic, gravity and geothermal data. In: Durand, B., Jolivet, L., Horváth, F., Serrane, M. (Eds.), *The Mediterranean Basins: Extension Within the Alpine Orogen*. Geological Society of London, Special Publications 156, pp. 215–250.
- Tilita, M., Matenco, L., Dinu, C., Ionescu, L., Cloetingh, S., 2013. Understanding the kinematic evolution and genesis of a back-arc continental “sag” basin: the Neogene evolution of the Transylvanian Basin. *Tectonophysics* 602, 237–258.
- Tilita, M., Scheck-Wenderoth, M., Matenco, L., Cloetingh, S., 2015. Reconstructing the coupled salt kinematics and subsidence evolution: numerical modelling inferences for the Miocene evolution of the Transylvanian Basin. *Tectonophysics* 658, 169–185.
- Tischler, M., Matenco, L., Filipescu, S., Gröger, H.R., Wetzell, A., Fügenschuh, B., 2008. Tectonics and Sedimentation During Convergence of the ALCAPA and Tisza-Dacia Continental Blocks: The Pienide Nappe Emplacement and Its Foredeep (N. Romania). *Geological Society, London*, pp. 317–334 Special Publications 298.
- Toljić, M., Matenco, L., Ducea, M.N., Stojadinović, U., Milivojević, J., Đerić, N., 2013. The evolution of a key segment in the Europe–Adria collision: the Fruška Gora of northern Serbia. *Glob. Planet. Chang.* 103, 39–62.
- Turcotte, D.L., Schubert, G., 2002. *Geodynamics*, second edition. Cambridge University Press (472 pp.).
- Tzortzis, M., Tsertos, H., 2005. Natural radioelement concentration in the Troodos Ophiolite Complex of Cyprus. *J. Geochem. Explor.* 85, 47–54.
- Van Wees, J.D., van Bergen, F., David, P., Nepveu, M., Beekman, F., Cloetingh, S., Bonté, D., 2009. Probabilistic tectonic heat flow modeling for basin maturation: Assessment method and applications. *Mar. Pet. Geol.* 26, 536–551.
- Velicic, S., Visarion, M., 1984. Geothermal models for the East Carpathians. *Tectonophysics* 103, 157–165.
- Vissers, R.L.M., 2012. Extension in a convergent tectonic setting: a lithospheric view on the Alboran system of SW Europe. *Geol. Belg.* 15, 53–72.
- von Quadt, A., Moritz, R., Peytcheva, I., Heinrich, C.A., 2005. 3: geochronology and geodynamics of Late Cretaceous magmatism and Cu-Au mineralization in the Panagyurishte region of the Apuseni-Banat-Timok-Srednogorie belt, Bulgaria. *Ore Geol. Rev.* 27, 95–126.
- Ziegler, P.A., Schumacher, M.E., Dezes, P., Van Wees, J.D., Cloetingh, S., 2006. Post-Variscan evolution of the lithosphere in the area of the European Cenozoic Rift System. *Geol. Soc. Lond. Memoir.* 32, 97–112.